Review

Progress in the Optical Sensing of Cardiac Biomarkers

Cristina Polonschii , Monica Potara , Madalina Iancu , Sorin David , Roberta Maria Banciu , Alina Vasilescu * , Simion Astilean

Posted Date: 12 May 2023

doi: 10.20944/preprints202305.0924.v1

Keywords: cardiovascular diseases; optical assay; biosensors

Review

Progress in the Optical Sensing of Cardiac Biomarkers

Cristina Polonschii [1,*], Monica Potara [2,*], Madalina Iancu [3], Sorin David [1], Roberta Maria Banciu [1,4], Alina Vasilescu [1,] and Simion Astilean [2]**

[1] International Centre of Biodynamics, Intrarea Portocalelor 1B, 060101, Bucharest, Romania; cpolonshii@biodyn.ro (CP); rbanciu@biodyn.ro (RMB), sdavid@biodyn.ro
[2] Nanobiophotonics and Laser Microspectroscopy Center, Interdisciplinary Research Institute in Bio-Nano-Sciences, Babes-Bolyai University, T. Laurian Str. 42, 400271, Cluj-Napoca, Romania; monica.potara@ubbcluj.ro, simion.astilean@ubbcluj.ro
[3] "Professor Dr. Agrippa Ionescu" Clinical Emergency Hospital, 7 Architect Ion Mincu Street, Bucharest, Romania; madalina.iancu@gmail.com
[4] Faculty of Chemistry, University of Bucharest, 4-12 "Regina Elisabeta" Blvd, 030018, Bucharest, Romania
* Equally contributing authors
* Correspondence: avasilescu@biodyn.ro

Abstract: Biomarkers play key roles in diagnosis, risk assessment, treatment and supervision of cardiovascular diseases (CVD). Optical biosensors and assays are valuable analytical tools answering the need for fast and reliable measurements of biomarkers levels. This review presents a survey of recent literature with a focus on the past 5 years. The data indicates continuing trends towards multiplexed, simpler, cheaper, faster and innovative sensing while newer tendencies concern minimizing the sample volume or using alternative sampling matrices such as saliva, for less invasive assays. The use of enzyme mimicking activity of nanomaterials gained ground in comparison to their more traditional roles as signaling probe, immobilization support for biomolecules or for signal amplification. The growing use of aptamers as replacements for antibodies prompted emerging applications of DNA amplification and editing techniques. Optical biosensors and assays were tested with larger sets of clinical samples and compared with the current standard methods. The ambitious goals on the horizon for CVD testing include the discovery and determination of relevant biomarkers with the help of artificial intelligence, more stable specific recognition elements for biomarkers and fast, cheap readers and disposable tests to facilitate rapid testing at home. As the field is progressing at an impressive pace the opportunities for biosensors in the optical sensing of CVD biomarkers remain significant.

Keywords: cardiovascular diseases; optical assay; biosensors

1. Introduction

Cardiovascular diseases (CVD) represent the leading cause of mortality and morbidity worldwide [1] being responsible for approximately 17.9 million deaths each year [2]. Moreover, during the last 30 years, the World Health Organization reported a gradual increase in the number of patients with CVD, not only in developed but also in developing countries [3]. Unfortunately, not only older people are affected by CVD, especially nowadays, when sedentarism, obesity, smoking, diabetes, stress, hypertension and many other risk factors are at high levels. Despite all the progress in the field of cardiology, mortality and morbidity in relation with cardiovascular diseases are still very high. There are continuous efforts made by professional organizations, authorities and by research institutes to improve primary prevention and to establish simple algorithms in order to facilitate an early and accurate diagnosis of cardiovascular diseases.

The most frequent and life-threatening cardiac pathologies are acute and chronic coronary syndromes and heart failure, accounting for more than 75% of all cardiac emergency room presentations and hospitalizations. "Classical" or newer investigations are used in order to obtain a rapid and precise diagnosis and staging in every case.

After medical history and clinical examination, most cases presenting dyspnea, fatigue, leg swallowing or/and chest pain usually perform an electrocardiogram (ECG), blood tests, a chest

 doi:10.20944/preprints202305.0924.v1

radiography and an echocardiography as soon as possible. Depending of these results, several patients need further, more or less invasive tests such as: ECG or echocardiography stress test, coronary calcium score quantification by computer tomography (CT), coronary CT angiography, 24 hours ECG monitoring, chest CT, cardiac magnetic resonance, coronary angiography or cardiac catheterization. These are the main tests used by cardiologists in order to establish an accurate diagnosis and an adequate therapeutic approach [4,5]. Cardiac biomarkers of CVD play key roles in diagnosis, risk assessment, treatment, and supervision. The blood levels of cardiac troponin I (cTnI) and blood natriuretic peptides (BNP or NT-proBNP) are the most useful indicators for diagnosing both ischemic heart disease and heart failure. They are equally useful for evolution monitoring and treatment adjustment. Specific analytical tests are available in every emergency room and Cardiology department. However, they are far from being perfect, due to a variable percent of false positive or false negative tests and sometimes due to the duration of obtaining results, in relation with the high level of emergency in some cases.

The methods currently used in clinical laboratories exploit the selectivity and strong affinity binding between an antigen (i.e., the biomarker) and an antibody. The specific recognition event is translated into a chemiluminescence, fluorescence, colorimetric or radiometric signal. Various robust, ultrasensitive methods and bench top equipment are available in clinical laboratories and are complemented by simpler, point of care tests and devices available commercially and used in hospitals and care centers [6]. Nonetheless, there is place for further improvement of specificity, sensibility or speed of methods for cardiac biomarkers and for less invasive determinations, in the benefit of a very early diagnosis and best treatment for all patients.

Along with standard, laboratory- based methods for the biochemical analysis of a panel of cardiac biomarkers, various point of care devices, including based on biosensors have been proposed for the diagnostic and monitoring of cardiovascular diseases (CVD).

Biosensors are promoted as a solution for rapid, specific and cost-effective analysis, amenable for on site or point of care (POC) analysis and addressing various complex biological matrices, including e.g., saliva for non-invasive testing. As per 2020 data [7], the analytical performances of POC devices approach those of standard methods used in centralized laboratory settings, however documented proof of performance for whole blood analysis and randomized clinical trials were still needed to validate these devices as real alternatives to currently used methods.

The present work reports on the advances in optical biosensors for CVD developed in the past 5 years, placing an emphasis on selected CVD biomarkers. The main aim is to highlight several original approaches that may guide or inspire a researcher pursuing the development of new detection methods for CVD biomarkers. In addition, the review discusses the remaining challenges and the perspectives in this field.

The focus on optical detection methods is justified by the competitive advantage in comparison with other detection modes with equally great sensitivity (e.g, electrochemical [8,9]). Specifically, optical devices are compatible to either existing equipment or low-cost solutions, e.g., enabling their integration with smartphone detection or with the widely used lateral flow devices.

In optical biosensors, the biological recognition event where a CVD biomarker is bound to a specific antibody, aptamer, peptide, cell etc is detected by changes in the input light, which manifests as changes in the amplitude, the frequency, phase or polarization. There are five categories of optical biosensors based on photoluminescence (fluorescence in particular), chemiluminescence, colorimetry, spectroscopy methods (Surface enhance Raman spectroscopy and Infrared spectroscopy) and surface plasmon resonance (SPR) as detection modes. Electrochemiluminescence, where the optical readout relies on luminescence generated via an electrochemical process combines specific features of electrochemical and optical methods and will be discussed as well.

Various biomarkers have been proposed in relation to CVD diagnosis and monitoring [10]. A pragmatic overview of biosensors for CVD, from a medical professionals' angle, lists cardiac Troponin I (cTnI), brain natriuretic peptide (BNP), its precursor N-terminal proBNP (NT-proBNP) and D-dimer as the most useful CVD indicators [6]. Undoubtedly, there are many other compounds which, even if less specific by themselves help establish the risk or next steps in the treatment for a

 doi:10.20944/preprints202305.0924.v1

CVD patient. Multiplexed detection of cardiac biomarkers, a trend in the recent years [9], has higher accuracy for CVD diagnostics than single tests alone. Consequently, several additional biomarkers will be briefly discussed in this work, in particular myoglobin, creatinine kinase myocardial band (CK-MB, an isoform of creatinine kinase) and C-reactive protein (CRP).

The effervescence in the field of POC devices is manifested in various directions of development, from monitoring heart failure patients at home (e.g., a lateral flow immunoassay (LFIA) for NT-proBNP coupled with portable reader and with IoT implementing[11]) to non-invasive monitoring tools to be used in emergency service vehicles or emergency (e.g., a transdermal device for the detection of cardiac troponin by Attenuated Total Reflection Fourier Transformed Infrared Spectroscopy (ATR-FTIR) [12]). Where do optical biosensors fit in this landscape? To answer this question, the main features and analytical performances of optical biosensors developed in the past 5 years are discussed further below in relation to the detection method.

2. CVD Biomarkers

The first biomarker released after the damage occurs to myocardial muscle cells is myoglobin. Myoglobin was indicated to be a potential biomarker for AMI, the maximum quantity after myocardial cell death being produced within 4 to 6 hours from the infarction event [13]. In this interval the myoglobin levels in blood rise to 70 - 200 ng/mL, while normal values are reported to be 6-85 ng/mL [14]. If the patient's blood is analyzed after this period of time, the concentration of myoglobin is no longer relevant as it reverts to its base value. Moreover, myoglobin concentration it is not a very specific CVD indicator, it can rise when other medical conditions occur, such as inflammation, renal failure or skeletal muscular dystrophy [15].

B-type natriuretic peptide (BNP), cardiac troponin I (cTnI), and C-reactive protein (CRP) are released after myoglobin and are specific markers for coronary events. BNP is useful for the diagnosis of heart failure (HF) and for the prognosis in patients with acute coronary syndrome (ACS). CRP is an important prognostic indicator of cardiovascular risk and ACS. Cardiac troponin I, cTnI has become a standard marker for the detection of acute myocardial infarction (AMI). During the heart infarction, the cardiac troponin T (cTnT) is immediately released to the bloodstream. The N-Terminal portion of the B-type natriuretic peptide (NT-proBNP) is a sensitive marker for assessing the risk of heart failure risk. Elevated concentrations of these cardiac markers in serum are associated with recurrent CVD events and higher death rates [16].

Historically, cardiovascular diseases were primarily diagnosed from ECG using graphical abnormalities and elevated quantities of cardiac muscle enzymes, namely CK-MB. Creatinine kinases are enzymes that catalyze the transfer of a phosphate group from creatinine phosphate to adenosine diphosphate, thus leading to the formation of adenosine triphosphate. The enzyme is the combination of two subunits named "M" and "B" which give the complete name "CK-MB". The normal percentage of total creatinine kinase is 3-5%, while the peak level ranges from 15 to 30% within 3 to 8 hours from the myocardial cell wall injury event [17].

After it was established that some AMI suffering patients did not have increased serum levels of CK-MB, it was essential to find another biological marker. In muscle fibers, actin and myosin filaments interact in order to trigger the muscle contraction. Because this process is mediated by the troponin-tropomyosin complex, troponin proteins were taken into consideration as cardiac biomarkers. More specifically, serum troponin I (cTnI) was shown to be efficient in diagnosis of cardiac damage [18,19].

CVDs can have an inflammation component and several biomarkers were proposed to be relevant in this respect, for instance tumor necrosis factor alpha (TBFα), interleukin-6 (IL-6) and C-reactive protein (CRP) [20].

Elevated basal levels of CRP in blood serum might indicate hypertension and high risk of CVD. The normal concentration of CRP is 10 mg/L, but when severe inflammation exists in the body, the value can be about 200 mg/L [21]. CRP is released after myoglobin and returns to normal blood levels after 19 hours following the acute inflammation event [21].

Preprints (www.preprints.org) | NOT PEER-REVIEWED | Posted: 12 May 2023 doi:10.20944/preprints202305.0924.v1

BNP has several biological effects, including decreased vascular resistance, dilation of blood vessels, decreased blood volume and pressure through increasing urine production. These effects are linked to BNP's release upon myocardial stretching [22]. BNP is produced from the enzymatic cleavage of proBNP precursor molecule, together with NT- proBNP, which is physiologically inactive [23]. The normal level of BNP in blood is around 20 pg/mL and increases in pathological events up to 0.1 ng/mL. The lifetime of BNP in blood is only 20 min. The quantity of NT-proBNP in the bloodstream is 5-10 times higher than the amount of BNP [24]. BNP and NT-proBNP are both considered excellent indicators of heart failure.

IL-6 is an inflammatory biomarker which is involved in regulating cell processes such as proliferation, differentiation and maturation. Congestive heart failure and left ventricular dysfunction are CVDs that are associated with increased concentrations of IL-6 [25]. The levels of IL-6 in blood evolve from less than 0.7pg/ml in healthy patients to up to 15 ng/mL in heart failure and can even reach 50 ng/ in case of severe inflammation [25-27].

TNFα is a cytokine, an intracellular chemical messenger involved in inflammatory processes. Even if this biomarker is not specific for CVDs, it predicts mortality in patients with heart failure**.** TNFα's normal range in serum is between 0.4 and 1 pg/mL, while levels of 1-10 pg/mL indicate heart failure and myocardial infarction [26,27].

3. Optical Biosensors for CVD: Recent Examples

3.1. SPR-Based Biosensors

Surface plasmon resonance (SPR) based assays were successfully used for the detection of numerous biomarkers in plasma and serum [28]. SPR is very sensitive to the refractive index and can be used to detect any molecule for which a ligand with high affinity such as an antibody or aptamer exists. Usually, the sensor surface is immobilized with a layer of specific antibody or aptamer ligand and the target molecule is injected over the surface. As the target molecules bind to the ligands, the refractive index changes proportionally to the accumulated mass or modifications in the structure of the active layer [29] and is detected and quantified by SPR. Most of current SPR detection schemes are based on angular or wavelength interrogation (by monitoring the shift of SPR dips), and on intensity interrogation (by monitoring the intensity under a fixed angle of incidence or wavelength). They have a typical resolution of 10^{-5}–10^{-7} refractive index units (RIU)[30], with the angle resolved-SPR having intrinsic higher sensitivity than single angle SPR [31]. However, angle-resolved SPR devices generally require expensive equipment, complicated optics, and precise alignment of the components, features that hinder the development of a portable device.

An SPR biosensor immobilized with anti-cardiac troponin I monoclonal antibody was developed by [32] and used for the detection of cTnI in aqueous solution and patient serum and kinetic analysis. The gold surface of the SPR chip was functionalized with polyacrylic acid and polydiallyldimethylammonium chloride. Using amino-coupling, the anti-cardiac troponin I monoclonal antibody was immobilized and then the SPR biosensor was blocked with BSA. The limit of detection and limit of quantification were calculated as 0.00012 ng/mL and 0.00041 ng/mL, respectively. The SPR measurements were performed using the commercial SPR imaging system GenOptics, SPRiLab (Orsay, France).

A strategy for cTnI detection was developed by constructing a universal biosensing interface composed of zwitterionic peptides and aptamers [33]. The peptides were self-assembled onto gold chips, some of them being biotinylated. The cTnI-specific biotinylated aptamers were immobilized via streptavidin-biotin system. A custom-made angle-scanning SPR system based on the Kretschmann configuration was used for measurements. The developed aptasensor had a linear detection range of cTnI from 20 ng/ml to 600 ng/ml and a detection limit of 20 ng/ml. Due to the antifouling property of the zwitterionic peptide, the developed aptasensor had a high resistance towards protein fouling.

Long-range surface plasmon-polariton (LRSPP) waveguides were used as biosensors for label-free detection of cTnI [34]. The sensors consist of 5-μm-wide 35-nm-thick gold stripes embedded in a

Preprints (www.preprints.org) | NOT PEER-REVIEWED | Posted: 12 May 2023 doi:10.20944/preprints202305.0924.v1

low-index optical-grade fluoropolymer (CYTOP) with fluidic channels etched to the Au surface of the stripes. Direct and sandwich assays were developed and demonstrated over the concentration range from 1 to 1000 ng/mL, yielding detection limits of 430 pg/mL for the direct assay and 28 pg/mL for the sandwich assay, the latter being physiologically relevant to the early detection or onset of AMI.

A nanoplasmonic biosensor chip was developed by [35] to assay cardiac troponin T (cTnT) in human biofluids (plasma, serum, and urine) with high specificity. The sensing mechanism is based on the adsorption model that measures the localized surface plasmon resonance (LSPR) wavelength shift of anti-cTnT functionalized gold triangular nanoprisms (Au TNPs) induced by change of their local dielectric environment upon binding of cTnT (Figure 1). Controlled manipulation of the sensing volume and decay length of Au TNPs together with the appropriate surface functionalization and immobilization of anti-cTnT onto TNPs allowed to achieve a limit of detection (LOD) of the cTnT assay at attomolar concentration (~15 aM) in human plasma.

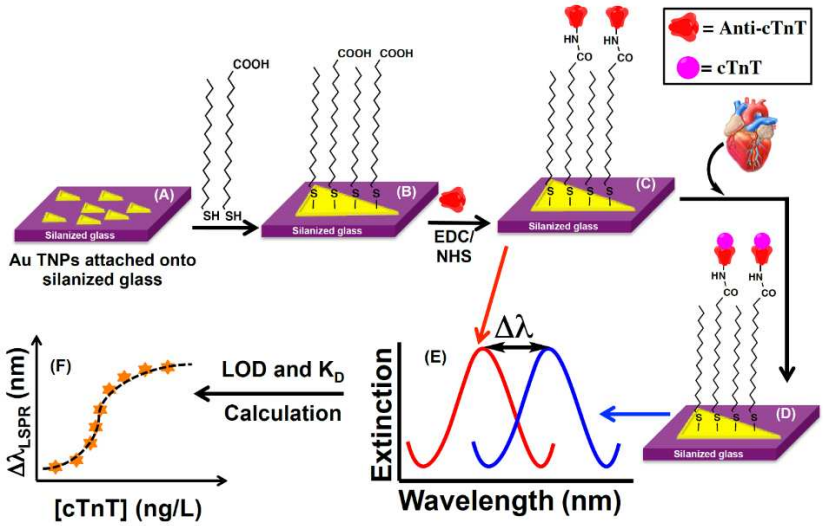

Figure 1. Design of a chip-based format LSPR cTnT biosensor. (A) Au TNPs attached onto silanized glass, (B) after being functionalized with a 1:1 mole ratio of 1-dodecanethiol and 16-mercaptohexadecanoic acid, (C) further functionalization with anti-cTnT through EDC/NHS amide coupling to complete the nanosensor, (D) detection of cTnT upon binding to anti-cTnT on sensor surface, (E) representation of nanosensor absorption maxima (λLSPR) peak shift before and after binding of cTnT, and (F) relationship between ΔλLSPR and cTnT concentration to calculate the LOD and KD. For simplicity, only one Au TNP is shown in the functionalization steps. Reproduced from [35] with permission from The Royal Society of Chemistry.

A biosensor based on a plasmonic exposed core optical fiber tip was developed for the rapid and label-free detection of the N-Terminal portion of the NT-proBNP [36]. The biosensor is based on a fiber tip covered with a gold layer, enabling SPR measurements that was functionalized with anti-NTproBNP antibodies. It was capable of monitoring NT-proBNP concentrations from 0.01 to 100 ng/mL, in a concentration range of clinical interest [36].

An ultrasensitive SPR immunoassay was developed for the specific detection of human cTnI. Based on the classical thin gold layer as the SPR sensing film, the surface was further modified by hollow gold nanoparticles (HGNPs) and polydopamine (PDA) sequentially, and then was immobilized with antibodies for specific recognition of target analyte. The interaction between the localized surface plasmon resonances of HGNPs and the propagating plasmon on the surface of the gold film leads to the amplification of SPR response signal. For additional sensitivity increase the sample was incubated with specific magnetic probes made of PDA-wrapped magnetic multi-walled carbon nanotubes (MMWCNTs-PDA) conjugated with detection antibodies (dAb). The magnetically assisted extraction of the target from the sample overcomes the disadvantage of slow diffusion

 doi:10.20944/preprints202305.0924.v1

limited mass transfer and matrix interference, reducing the nonspecific interferences while detecting cTnI in human serum. The combination of the above improvements results in the significant sensitivity enhancement of the SPR immunoassay. The concentration of cTnI with minimum detectable SPR response obtained by the assay was 1.25 ng/mL [37].

One study lead by Zhao [38] achieved the detection of BNP in serum samples using aptamer-functionalized Au nanoparticles (GNPs-Apt) and antibody-modified magnetoplasmonic nanoparticles (MNPs-Ab) for dual evaluation. Both types of nanoparticles (NPs) specifically recognize BNP in order to form magnetoplasmonic nanoconjugates (NCs). Avoiding degradation is critical for analysis, so applying an external magnetic field makes possible the separation of the analyte from the complex samples. Next the recognition of NCs is carried out by complementary-DNA (cDNA) of the aptamer immobilized on the gold film of SPR chip (Figure 2). Therefore, the refractive index of the gold surface significantly modifies due to strong electronic coupling between MNPs and the surface plasmon wave of GNPs. The linear range obtained with this method is from 0.1 pg/mL to 100 pg/mL and the limit of detection equals 28.2 fg/mL. The selectivity matter was addressed using some proteins and molecules as interfering substances, bovine hemoglobin (BHb), ascorbic acid (AA), myoglobin (Myo), ovalbumin (OVA) and bovine serum albumin (BSA). Regarding real sample analysis, the group investigated the feasibility of the SPR biosensor in spiked serum. The recoveries were between 92.5-113.9 %, with RSDs lower than 15 %, indicating great accuracy for BNP sensing by the developed SPR method.

In another study by Harpaz [39], an SPR chip was designed and used in a novel point-of-care SPR system for the detection of the stroke biomarkers NT-proBNP and S100β in water and plasma samples. The POC system was based on the commercial PhotonicSys SPR H5 from PhotonicSys (Neveh Shalom-Wahat Alsalam, Israel, www.photonicsys.com). The SPR chip had a bimetallic composition consisting of 30 nm silver and 15 nm gold. The chip was functionalized with thiols and then the specific antibodies for the target biomarkers were immobilized by amino-coupling. NT-proBNP and S100β were detected in a range of clinically relevant concentrations for stroke, from 0.1 ng/mL to 10 ng/mL.

In conclusion, SPR based biosensors are able to detect CVD biomarkers in a label-free and fast manner. Moreover, these biosensors can be implemented in point-of-care (POC) devices due to their versatility, long-term stability, and simple concepts. Amongst the various SPR detection methods, LSPR biosensors proved to be the most sensitive, with a LOD in attomolar range. Various enrichment techniques (adding affine or magnetic tags) may further improve the detection limit and reduce the nonspecific response of complex clinical samples.

Preprints (www.preprints.org) | NOT PEER-REVIEWED | Posted: 12 May 2023 doi:10.20944/preprints202305.0924.v1

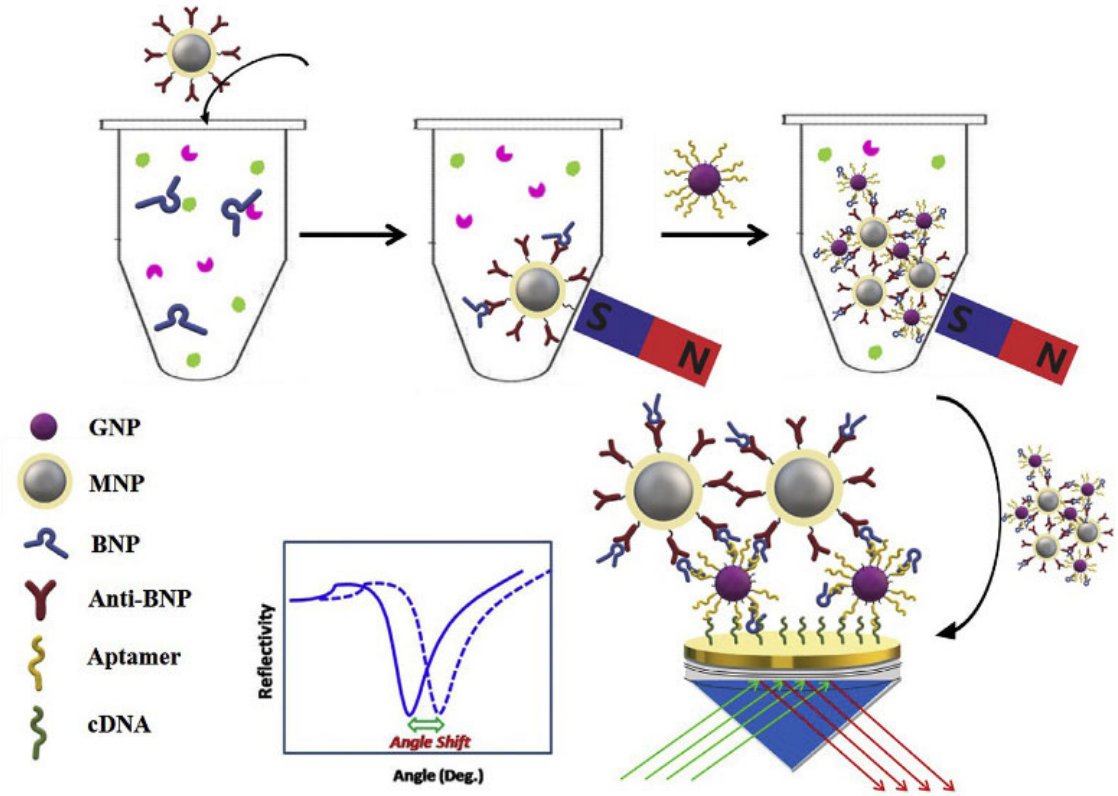

Figure 2. – Schematic of the BNP SPR sensing strategy via magnetoplasmonic nanocomposites for signal amplification. Reproduced from [38] with permission from Elsevier.

3.2. SERS Biosensors for Cardiac Biomarkers

Surface-enhanced Raman spectroscopy (SERS) combines outstanding features for sensing applications, such as specific identification and structural information about the molecular species based on their unique vibrational Raman fingerprint, as well as ultrasensitive detection down to a single molecule. SERS largely relies on collective oscillations of conduction electrons known as surface plasmon resonances that produce drastic amplification of the electromagnetic fields near the surface of noble-metal nanostructures. These, in turn, significantly enhance the Raman signal from the molecules placed in their close vicinity up to 10^8-10^{10} orders of magnitude through the so-called electromagnetic mechanism (EM). The molecules directly adsorbed on the nanostructured substrate can experience a charge transfer with the metal surface, leading to an additional enhancement of the Raman signal of 10^1-10^3 orders of magnitude through the so-called chemical charge transfer (CT) mechanism [40,41]. The SERS technique has been widely employed as a powerful tool in the development of sensing bioassays for the selective, sensitive and quantitative detection of various cardiac biomarkers. Some of the fabricated SERS bioassays involve the immobilization of the cardiac biomarkers onto nanostructured surfaces, followed by direct analysis and identification of their Raman spectral fingerprint. However, this strategy, called direct SERS detection suffers from low selectivity due to the multiple components found in the biological samples, which can interfere with the SERS signal of the biomarker of interest. This in turn complicates the data analysis and limits accurate biomarker quantification. Indirect SERS detection has been proposed as an alternative to direct detection to improve the selectivity of the assay and simplify the data analysis. For this, the SERS substrate is modified with Raman reporters and receptors to ensure the specific capture of the target biomarkers. SERS nanotags built on noble-metal nanoparticles conjugated with Raman reporters and specific receptors were also used to increase the selectivity of the assay and accomplish simultaneous determination of multiple target cardiac biomarkers.

The recent years witnessed the production and application in sensing of new nanomaterials for enhanced sensitivity of SERS detection, new strategies for the selective and accurate detection in

 doi:10.20944/preprints202305.0924.v1

biological samples, in the range relevant for diagnosing CVDs, multiplexed detection and increased use of portable equipment.

For example, nanomaterials like gold or silver nanoaggregates, core-shell plasmonic bimetallic nanoparticles, hybrid plasmonic-magnetic nanoparticles were coupled with specific bioreceptors (mainly antibodies) and Raman reporters like rhodamine-6G (R6G), nile blue A (NBA), malachite green isothiocyanate (MGITC), methylene blue (MB), 4-mercaptobenzoic acid (4-MBA) etc. for selective and ultrasensitive detection of several cardiac biomarkers. Different plasmonic nanoplatforms were fabricated and optimized for high sensitivity for either direct or indirect SERS detection of various cardiac biomarkers, including CRP [42], cTnI), B-type natriuretic peptide (BNP), CK-MB, Myo,NT-ProBNP, neutrophil gelatinase-associated lipocalin (NGAL), glycogen phosphorylase isoenzyme BB (GPBB), neuropeptide Y (NPY) and heart type fatty acid-binding protein (H-FABP). In the following are summarized several successful SERS biosensors for CVD, with the emphasis on the nanostructures' designs proposed for efficient sensing.

Benford et al. developed the first SERS assay to qualitatively analyze three cardiac biomarkers in diagnosing acute coronary syndrome [43]. Specifically, SERS active aggregated gold nanoparticles (AuNPs) trapped at the entrance of a nanofluidic device were used as sensing elements to detect BNP, cTn, and CRP. This sensing platform enables the detection and identification of BNP, cTn, and CRP at physiologically relevant concentrations. Unfortunately, no real sample analysis was reported in the work. A key issue in SERS-based detection bioassays represents the biosensor's capacity to detect the target analyte with high specificity. Given this, the same group designed an improved SERS bioassay for the specific detection of CRP [44]. The proposed platform incorporates agarose beads functionalized with an anti-CRP antibody for the specific capture of CRP, aggregated gold nanoparticles as the SERS units, and CRP labeled Rhodamine-6G (R6G) as a target analyte. Besides the specific detection of CRP, a correlation between the amount of CRP and the SERS signal of R6G was also observed. However, there was no validation of the results in clinical samples.

Knowing the concentration of cardiac biomarkers in human blood is essential in diagnosing cardiovascular diseases. Therefore, the efforts in designing SERS assays were focused not only on selective detection but also on the quantification of the biomarkers in blood samples. A good example is a study reported by Cong et al.[45]. In their work, the SERS technique and an enzyme catalysis bioassay (ELISA) were combined for selective and sensitive detection and quantification of the human cardiac isoform of troponin T, cTnT in human serum. The proposed detection strategy involves the use of citrate-capped spherical AuNPs as a SERS substrate, and the resulting product of the enzyme-catalyzed 3,3′,5,5′-tetramethylbenzidine reaction, TMB^{2+} as a SERS probe.

Remarkably, the developed biosensor achieved a broader linear concentration range (2 ~ 320 pg/ml) and an improved sensitivity (limit of detection -LOD of 2 pg/ml) compared with the UV-Vis technique (linear concentration range 4 ~ 80 pg/ml and LOD of 4 pg/ml). The performance of the sensor assay for clinical applications was evaluated with two serum samples containing two concentrations of cTnT, 16 and 8 pg/ml, respectively. The relative standard deviation for these two concentrations was 0.017 and 0.093 and the average recoveries were 100.01% and 86.815%, respectively. Cote and co-authors also exploited AuNPs to develop an optofluidic device for SERS detection of myoglobin [46]. The fabricated device comprising plastic plates, rubber layers, and a nanoporous membrane was exposed to a mixture containing rhodamine-6G (R6G) labeled myoglobin and colloidal AuNPs. The aggregation of AuNPs on the nanoporous membrane leads to the formation of a robust, sensitive and reproducible SERS active plasmonic substrate. The intensity variation of a characteristic Raman band of R6G was used to quantify myoglobin concentration in solution over a physiologically relevant range (1.2 nM to 30 nM). To further evaluate the performance of the assay in complex samples, bovine serum albumin (BSA) was introduced as a possible interfering compound. Unfortunately, a decrease of the SERS signal was noticed in the presence of BSA for all concentrations of myoglobin tested. Furthermore, no real sample analysis was provided in the work. Later, silver nanoaggregates were exploited by the same authors to fabricate a bioassay for SERS detection of the human cardiac Troponin I (cTnI) in solution [47]. In this system, silver nanoparticles (AgNPs) were first encoded with the Raman reporter molecule DTNB and then

 doi:10.20944/preprints202305.0924.v1

aggregated to give a strong and stable SERS signal. In the second step, the Ag nanoaggregates were encapsulated in a silica shell to stabilize them and facilitate their further bioconjugation. Finally, the core-shell Ag nanoaggregates-silica architecture was coated with polyethylene glycol (PEG) and functionalized with cTnI protein and BSA to endow them with an affinity for the cTnI antibody. Unfortunately, this study did not address the detection of cTnI and instead only examined the SERS signal of the nanoconjugate. 3D silver anisotropic nano-pinetree array modified indium tin oxide (Ag NPT/ITO) was proposed by El-Said and co-authors as an alternative to silver nanoaggregates to develop an ultrasensitive SERS platform for direct, label-free detection of myoglobin [48]. Another three Ag nanostructures/ITO substrates (Ag nanoaggregates/ITO, Ag nanorods/ITO and Ag nanobranched/ITO) were also prepared and compared with Ag NPT/ITO regarding their SERS performance. The fabricated Ag NPT/ITO substrate showed the best Raman signals, yielding a LOD of 10×10^{-9} g mL^{-1} and a wide working range for myoglobin quantification from 5×10^{-6} to 10×10^{-9} g mL^{-1}. The sensor performance for clinical applications was evaluated by analyzing urine samples spiked with a known amount of myoglobin. A linear relationship between the Raman intensity and the myoglobin concentration in urine over a range of 10 ng/mL to 5 μg/mL was obtained. In addition, the calibration curves for urine and buffer have almost the same slopes, demonstrating the accuracy of the detection without interferences. However, there was no validation of the results by parallel analysis using a standard method.

Ultrasensitivity and high specificity were also reported by Gao et al., who managed to design a novel hybrid microfluidic chip for simultaneous SERS detection of CK-MB and cTnI cardiac markers [49]. In this system, a SERS substrate fabricated by in-situ synthesis of AuNPs on the patterned paper microchannels was used as a capture platform, while AuNPs labeled with malachite green isothiocyanate (MGITC) Raman reporter molecules were employed as SERS detection nanotags. To achieve specificity toward CK-MB and cTnI, the SERS platform and the Raman probes were conjugated with capture and detection antibodies against CK-MB and cTnI. Selective quantification of CK-MB and cTnI was accomplished by measuring the SERS signal on a sandwich-type nanoarchitecture formed after the immune reaction, yielding a LOD of 7.92 pg mL^{-1} and 2.94 pg mL^{-1} for CK-MB and cTnI, respectively. However, some interfering SERS signal was noticed in the presence of BSA, thrombin, and PSA spiked in serum samples due to the non-specific adsorption of SERS nanotags on the detection area.

Core-shell plasmonic bimetallic nanoparticles have also been employed in the development of various SERS bioassay as they offer several advantages compared with monometallic nanoparticles, such as high stability and reproducibility of the Raman signal, as well as an increased SERS performance. Both, Raman reporter-labeled and reporter-embedded core-shell nanotags were prepared and exploited as ultrasensitive SERS nanoprobes for selective determination of cardiac biomarkers.

For instance, Bai et al. fabricated three classes of bimetallic core-shell SERS nanoprobes and one class of monometallic nanoprobe and investigated their SERS activity by experimental measurement and theoretical analysis [50]. The monometallic class was built on citrate-capped AuNPs-encoded with Nile blue A (NBA) dye. Two classes of the core-shell nanoprobes consist on a metallic core (Au or Ag) with a metallic shell (Ag or Au) and NBA embedded at their interface and also labelled at their surface. The other class of core-shell nanoprobes was built on Au-core labeled with NBA, a silver shell labeled with NBA and then etched with $HAuCl_4$ to form Au@AgAuNPs with nanometric gaps inside. The obtained Au@Ag-Au NPs were further encoded with NBA. Both experimental and theoretical results showed that Au@Ag-Au NPs exhibited the best SERS performance due to the strong electromagnetic field created in the nanogaps between the core and shell. Therefore, the authors have selected Au@Ag-Au NPs to develop a SERS-based lateral flow assay strips for selective, highly sensitive and quantitative analysis of cardiac troponin I (cTnI). To achieve specificity toward cTnI, the fabricated Au@Ag-AuNPs and test line were conjugated with detection and capture antibodies, respectively. Quantification of cTnI was performed by monitoring the SERS intensity of a characteristic Raman band of NBA in a sandwich immunocomplex formed after exposure of the sample pad to various concentrations of cTnI. The designed SERS-based lateral flow assay strips

 doi:10.20944/preprints202305.0924.v1

provide reproducible, selective and high-sensitive detection of cTnI with the LOD of 0.09 ng mL^{-1}. Even though no interference signal was found when CRP, BNP, Myo, and CK-MB were present, real sample analysis was unfortunately not addressed in this study.

Zhang et al. also exploited the core-shell SERS nanotags to develop a SERS-based lateral flow assay strips for simultaneous detection of Myo, cTnI and CK-MB on three test lines [51]. In their design, SERS nanotags were built on an Ag core with an Au shell and NBA Raman reporter molecules embedded at their interface. The fabricated SERS nanotags were then conjugated with detection antibodies of three biomarkers to form an immunocomplex with the capture antibodies on a nitrocellulose membrane when the target biomarkers are present. The intensity of the SERS spectra recorded from the three test lines at 785 nm laser excitation was used for quantitative analysis of Myo, cTnI, and CK-MB. The designed SERS-based lateral flow assay provides reproducible, high-sensitive and multiplex detection of Myo, cTnI and CK-MB with a wide linear dynamic range and the LODs of 3.2, 0.44, and 0.55 pg mL^{-1}, respectively. The diagnostic performance of the assay was evaluated with 50 serum samples collected from hospitalized patients suffering from AMI and the results were compared with the FDA approved clinical chemiluminescence immunoassay (CLIA) method. Passing- Boblok regression and Spearman's rank correlation coefficient were used to examine the linear dependence between the two methods. A good linear correlation of the two methods was obtained. The assay has better sensitivity than CLIA, is low-cost and easy to use and requires 15 min per marker. However, the developed sensor has speed constraints, necessitating the examination of three test lines. Thus, shortly thereafter, the same group reported an improved version of the SERS-based lateral flow assay for rapid, multiplex quantitative detection of CK-MB, cTnI, and Myo using a single test line [52]. In their design, three different SERS nanotags, namely methylene blue (MB), nile blue A (NBA) and rhodamine 6 G (R6 G) were built on an Ag core with an Au shell and Raman reporters embedded at their interface. The SERS spectra recorded from a single test line at 785 nm laser excitation show distinct features for all corresponding nanotags of biomarkers. The designed sensor yielded a LOD of 0.93, 0.89, and 4.2 pg mL^{-1} and linear dynamic range of 0.02–90, 0.01–50, and 0.01–500 ng mL^{-1} for CK-MB, cTnI, and Myo, respectively. Five human serum samples from hospitalized patients with AMI were examined to ascertain whether the assay is suitable for usage in clinical settings. The CLIA approach was used to compare the outcomes. Real samples yielded very good recoveries, ranging from 86.7% to 113.5%, demonstrating the accuracy of the assay.

Yu et al. also developed a core-shell SERS nanotag-based sandwich immunoassay for rapid, sensitive and simultaneous detection of cTnI and CK-MB [53]. The sandwich system was based on Au@Ag core–shell nanoparticles conjugated with malachite green isothiocyanate (MGITC) and polyclonal antibodies as the SERS detection element and a gold-patterned chip functionalized with monoclonal antibodies as the SERS active template. The designed assay enabled quantitative analysis of cTnI and CK-MB with a LOD of 8.9 pg mL^{-1} and 9.7 pg mL^{-1} for cTnI and CK-MB, respectively. The clinical applicability of the sensor was evaluated with 5 serum samples collected from patients with AMI and the results were compared with those obtained with a commercially available chemiluminescence assay. The concentrations of cTnI and CK-MB determined by the SERS-based assay were comparable to those determined by the chemiluminescence technique, and they were all within the clinically acceptable range. Another approach for ultrasensitive simultaneous detection of cTnI, N-terminal prohormone of brain natriuretic peptide (NT-ProBNP) and neutrophil gelatinase-associated lipocalin (NGAL) was reported by Zhu and co-authors [54]. Their strategy involves using bimetallic Ag-Au nanostars conjugated with Raman reporters (4-mercaptobenzoic acid (4-MBA), 5′-dithiobis-(2-nitrobenzoic acid) (DTNB), 2-naphthalenethiol (NT)) and detection antibodies as SERS nanotags and a three-dimensional ordered macroporous Au-Ag-Au plasmonic array conjugated with capture antibodies as a substrate. to improve the reproducibility and sensitivity of the assay. The sensitivity of the system is achieved through the formation of Raman hot-spots between nanotags and substrate after the biomolecular recognition. This SERS-based sandwich immunoassay allowed for sensitive and reproducible multiplex detection, yielding a LOD of 0.76, 0.53 and 0.41 fg mL^{-1} for cTnI, NT-ProBNP and NGAL, respectively. The suitability of the developed immunoassay for clinical applications was also demonstrated by simultaneous determination of cTnI, NT-ProBNP and NGAL

Preprints (www.preprints.org) | NOT PEER-REVIEWED | Posted: 12 May 2023 doi:10.20944/preprints202305.0924.v1

in human serum samples. The results were compared to those obtained using the dot immunogold filtration test (DIGFA) in order to confirm the accuracy of the immunoassay. The two techniques' agreement was found to be reasonable, thus proving the potential of the proposed sensor for clinical applications.

Raman reporter-embedded Au nanorod-core Au-shell nanotags were employed by Khlebtsov et al. for the design of a SERS-based lateral flow immunoassay for fast, sensitive, semiquantitative determination of cTnI [55]. Detection of cTnI was performed by Raman mapping of the test zone, while quantification was achieved by monitoring the SERS intensity of a specific band of 1,4-nitrobenzenthiole (NBT) Raman reporter following the exposure of NPs to different concentrations of cTnI, reaching a LOD of 0.1 ng mL^{-1}. However, the selectivity of the assay and analysis of the real samples were not reported in this work. Going one step forward, Tu et al. have recently employed gap-enhanced nanoparticles (GeNPs) as ultrasensitive SERS nanotags to design a paper-based immunoassay for simultaneous quantification of three myocardial infarction biomarkers: cardiac troponin I (cTnI), copeptin, and heart-type fatty acid-binding protein (h-FABP) [56]. As schematically illustrated in Figure 3, GeNPs consist of three different SERS tags (4-mercaptophenylacetic acid (MPAA), 2,3,5,6-tetrafluoro-4-mercaptobenzoic acid (TFMBA) and 5,50-dithiobis(2-nitrobenzoic acid) (DTNB)) built on Raman reporter-embedded gold-core gold-shell with nanometric-size gaps of 0.9-1.1 nm created at the interface of the core-shell nanoarchitecture.

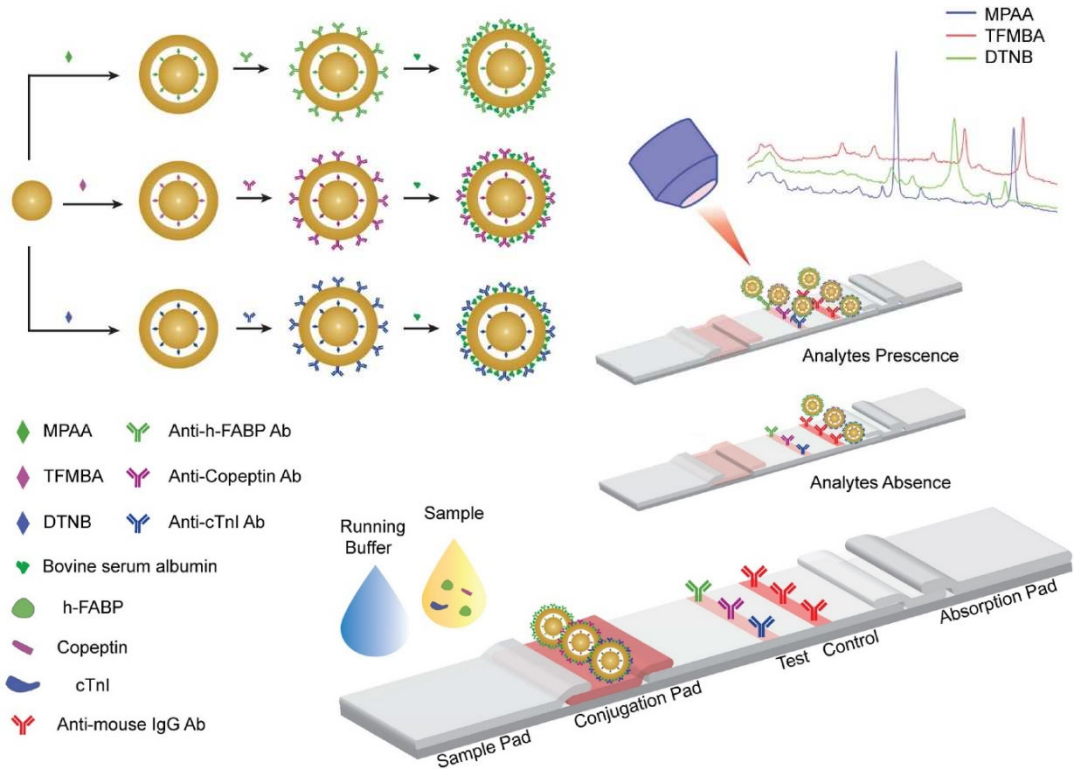

Figure 3. Schematic illustration of the process to prepare antibody conjugated gap-enhanced nanoparticle, and the lateral flow strip for a multiplex detection of the biomarker panel for myocardial infarction. Reprinted with permission from [56]. Copyright (2022) Elsevier.

Due to the high electromagnetic enhancement of the Raman signal inside the narrow nanogaps, GeNPs enabled an increase of the SERS signal by 105-250 times compared to the Au core. To achieve specificity toward the three target biomarkers, the fabricated GeNPs-based SERS nanotags were conjugated with detection antibodies against cTnI, copeptin and h-FABP (Figure 3). A single test line consisting of a nitrocellulose membrane conjugated with capture antibodies specific to cTnI, copeptin and h-FABP was used. A sandwich immunocomplex was formed on the test line only when the target biomarkers were present. The SERS spectra recorded from the test line at 780 nm laser excitation exhibited distinct SERS features related to each target biomarker, thus allowing the simultaneous

 doi:10.20944/preprints202305.0924.v1

detection, spectral discrimination and quantification of cTnI, copeptin and h-FABP with a LOD of 0.01 ng mL^{-1}, 0.86 ng mL^{-1}, 0.004 ng mL^{-1} for cTnI, h-FABP, and copeptin, respectively. Notably, the developed paper-based SERS assay enabled quantification of the three biomarkers in human serum samples in a clinically relevant range of concentrations. However, the sensor has some limitations due to the non-specific binding between the three different GeNP/antibody particles, biomarkers, and primary antibodies, which leads to some interference in the multiplex immunoassay.

Even though core-shell bimetallic (Au@Ag or Ag@Au) nanoparticles were extensively employed in several types of SERS bioassays, Tu et al. have proposed gold-core silica-shell nanoparticles as SERS nanotags to design a stable, reproducible and cost-effective aptamer-based sandwich assay on a paper strip for determination of cTnI *via* surface-enhanced resonance Raman spectroscopy (SERRS) [57]. In the developed design, spherical AuNPs with a diameter of 60 nm were first encoded with the Raman reporter molecule malachite green isothiocyanate (MGITC) and then encapsulated in a silica shell. For specific recognition of cTnI, the core-shell nanoparticles were functionalized with a secondary aptamer of cTnI, while the test line was modified with a primary aptamer of cTnI. The specific molecular interaction of aptamers and cTnI results in a sandwich architecture between the core-shell nanoparticles and the test line. Selective and sensitive detection of cTnI was accomplished by measuring the SERRS signal of the test line under resonant excitation at 638 nm, reaching a detection range of 0.016 to 0.1 ng ml^{-1}, with a LOD of 0.016 ng ml^{-1}. The suitability of the developed aptamer-based paper strip assay toward clinical applications was demonstrated by SERRS detection and quantification of cTnI in serum samples. Recovery factors were evaluated by spiking cTnI at 0.03 and 0.05 ng⁄ml in human serum without any treatment. The obtained values, in the range of 93.8% to 95.8% indicated the good accuracy of the method. Furthermore, the aptamer-based paper strip assay showed good stability after 10 days of storage at room temperature. However, the assay remains to be confirmed by parallel analysis with a larger sample set and a standardized technique.

Raman-encoded gold or silver nanoparticles enveloped in a silica shell were also employed by Lim et al. as extrinsic SERS probes to design a microfluidic paper-based device (μPAD) for simultaneous quantitative SERS measurement of three cardiac biomarkers: glycogen phosphorylase isoenzyme BB (GPBB), cTnI and creatine kinase-MB isoenzymes (CK-MB) [58]. The proposed bioassay ensured high reproducibility and ultrasensitivity to detect the three cardiac biomarkers with a LOD of 8, 10, and 1 pg mL^{-1} for GPBB, CK -MB and cTnT, respectively, showing high accuracy even in the detection of clinical samples of human serum. The results were further validated by a laboratory reference method, Siemens Centaur XPT Immunoassay System. Additionally, a predictive model was created to estimate the unknown concentration of cardiac biomarkers in serum samples and eliminate the standard calibration curves. A good fit of the predicted and experimental data was obtained.

Combining plasmonic substrates with magnetic nanoparticles has brought new advantages in SERS detection of cardiac biomarkers, enabling an increased sensitivity and a simple analysis procedure after magnetic separation. For example, a fast and sensitive SERS-based competitive immunoassay for the simultaneous detection of cTnI and CK-MB was demonstrated by Choo et al. [59]. Their method involves the use of magnetic beads functionalized with monoclonal antibodies for cTnI and CK-MB as capture agents and two different SERS nanoprobes based on hollow gold nanospheres conjugated with Raman reporters and cTnI and CK-MB antigens as SERS sensitive platforms for cTnI and CK-MB recognition. The proposed detection strategy involves the competitive interaction of free target antigens and antigen-conjugated SERS nanoprobes with monoclonal antibodies on magnetic beads, followed by magnetic separation and SERS analysis of the supernatant. The results showed that the developed SERS-based competitive immunoassay achieves a 100 to 1000-fold increase in sensitivity compared to electro-chemiluminescent assay, yielding a LOD of 42.5 pg mL^{-1} and 33.7 pg mL^{-1} for CK-MB and cTnI, respectively. The agreement of the two analytical methods was validated with Bland–Altman analysis and Passing–Bablok regression analysis. Remarkably, the fabricated SERS-based competitive immunoassay enables simultaneous quantitative detection of cTnI and CK-MB in patient serum at a single excitation wavelength.

 doi:10.20944/preprints202305.0924.v1

Another study uses metal-organic frameworks (MOFs)@Au Tetrapods (AuTPs) immobilized toluidine blue as the SERS tag, and Au nanoparticles functionalized $CoFe_2O_4$ magnetic nanospheres ($CoFe_2O_4$@AuNPs) as the purification and signal amplification agents to develop a highly efficient SERS-based sandwich immunosensor for ultrasensitive detection of N-terminal pro-brain natriuretic peptide (NT-proBNP) [60]. The fabricated SERS immunosensor enables specific capture of NT-proBNP *via* antigen-antibody immunoreaction, yielding a wide linear range for NT-proBNP quantification from 1 fg mL^{-1} to 1 ng mL^{-1} and a LOD of 0.75 fg mL^{-1}. Good recovery factors, in the range of 90.66% to 105.1% were obtained in human real serum samples, confirming the accuracy of the method. However, the results remain to be verified through parallel analysis with a standard commercially available technique.

Recently, Zheng et al. also employed $CoFe_2O_4$@AuNPs conjugated with specific antibodies to ensure the magnetic purification of the analytes and improve the sensitivity of their microfluidic immunosensor developed for specific SERS detection of brain natriuretic peptide (BNP) cardiac biomarker [61]. Apart from CoFe2O4@AuNPs, a SERS substrate consisting of metal–organic framework and Au-HEPES coupling nanoparticles (AuHPs) conjugated with toluidine blue and antibody against BNP was also introduced to further enhance the Raman signal of the sensor. Specific quantitative detection of BNP was performed by measuring the SERS signal with a portable Raman spectrometer based on a sandwich approach. The proposed immunosensor exhibited high stability, portability and ultrasensitivity, yielding a LOD at a level of pg mL^{-1}. However, the performance of the immunoassay in clinical samples was not reported in the study. A highly sensitive SERS-based immunoassay for selective quantitative detection of cTnI has been demonstrated by Fu and co-authors [62]. The fabricated immunosensor is composed on antibody/Raman reporter conjugated AuNP–functionalized graphene oxide as the SERS nanotags and signal amplification elements, and antibody modified magnetic beads as the capture probe and separation agents. By exploiting the high SERS performance of graphene oxide/AuNPs and strong binding chance between cTnI and the GO/AuNP an ultrasensitive analysis of cTnI is achieved with the LOD of 5 pg mL^{-1} and a linear range of detection from 0.01 to 1000 ng mL^{-1}. The suitability of the designed SERS immunoassay for practical applications was also demonstrated by the determination of TnI in serum substitute media. However, the results remain to be confirmed in clinical samples and compared with those obtained with a standard technique.

Wen et al. have demonstrated an innovative, portable reusable accurate diagnostics (PRADA) SERS-based immunoassay for simultaneous quantitative detection of troponin I (cTnI) and neuropeptide Y (NPY) in a microfluidic platform [63].

Preprints (www.preprints.org) | NOT PEER-REVIEWED | Posted: 12 May 2023 doi:10.20944/preprints202305.0924.v1

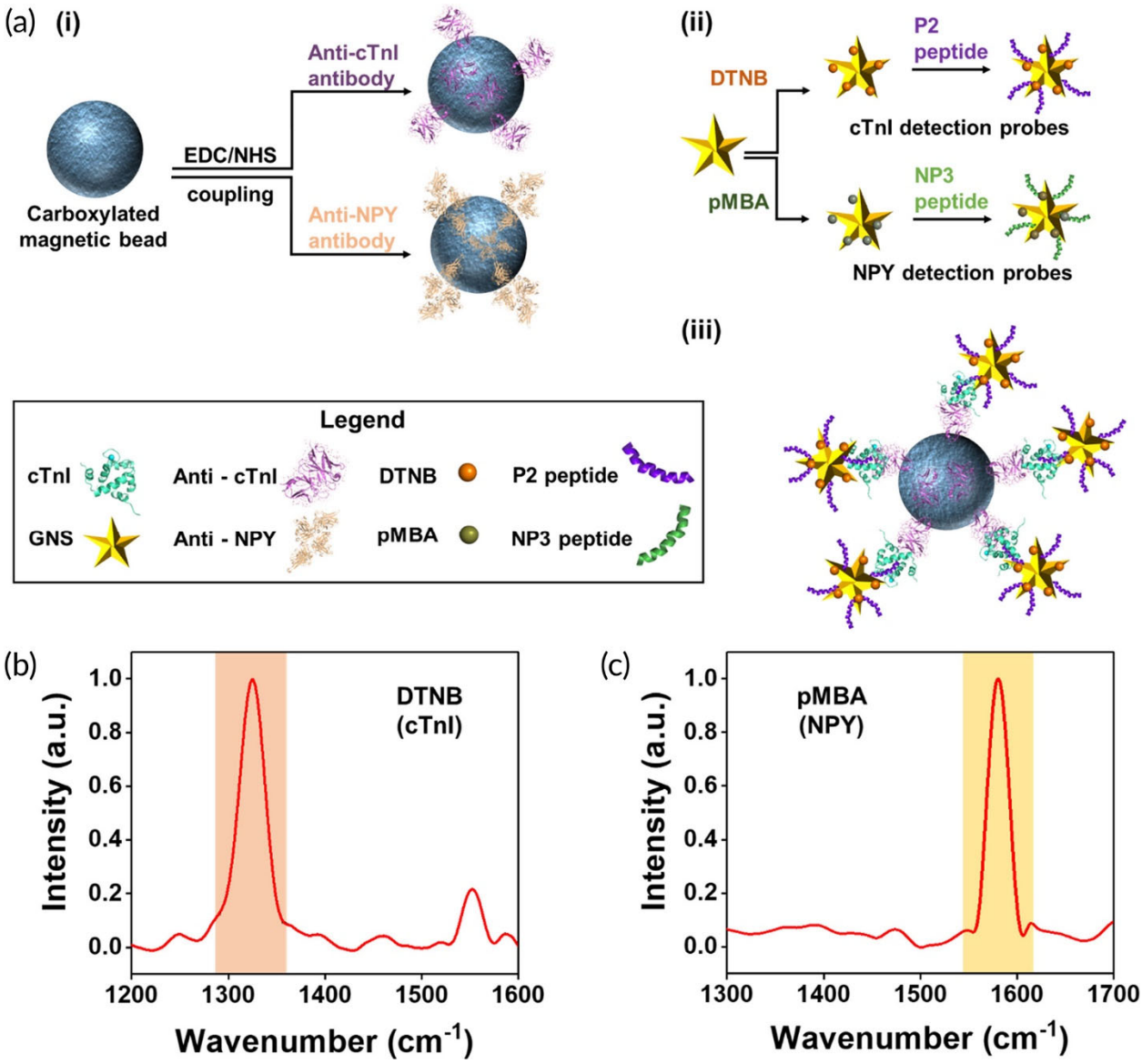

Figure 4. Fabrication of PRADA. (a) Schematic of the synthesis of capture and detection probes. (i) Magnetic beads functionalized with pAbs as capture probes. (ii) GNSs conjugated with SERS barcodes and peptide BREs as detection probes. (iii) The representative complete immunocomplex formed by capture probes, target antigens, and detection probes. (b, c) Normalized Raman spectra of GNSs functionalized with DTNB (1,325 cm−1) and pMBA (1,580 cm−1) for cTnI and NPY detection, respectively; the signature peaks are highlighted. BREs, biorecognition elements; GNSs, gold nanostars; pAbs, polyclonal antibodies; PRADA, portable reusable accurate diagnostics with nanostar antennas; SERS, surface enhanced Raman spectroscopy. Reprinted with permission from [63]. Copyright (2020) John Wiley & Son.

As illustrated in Figure 4a, antibody-conjugated magnetic beads were used as the capture platform, while SERS nanotags based on gold nanostars labeled with two different Raman reporters and peptide biorecognition elements were introduced as SERS detection probes. The SERS spectra recorded from the sandwich-type-immunocomplex at 785 nm laser excitation show the distinct features of the two nanotags corresponding to cTnI and NPY (Figure 4b). Specifically, the SERS intensity of DTNB at 1325 cm^{-1} was used for cTnI quantification, while NPY determination was accomplished by monitoring the SERS signal of pMBA at 1580 cm^{-1}. The PRADA sensing device exhibited high sensitivity, achieving a LOD comparable with the commercially available test kits: 0.0055 ng ml^{-1} and 0.12 ng ml^{-1} for cTnI NPY, respectively. Moreover, the sensor chip can be regenerated, thus being reusable for multiple detection cycles. Remarkably, the developed PRADA

assay showed high accuracy and reproducibility on evaluating cTnI in cardiac patient serum achieving limit of quantification (LOQ) of ≥0.03 ng/ml which is comparable to commercial assay and lower than many troponin immunoassays reported in the literature. Furthermore, the clinical performance of the PRADA assay was validated by parallel measurements with the ABBOTT ARCHITECT chemiluminescence assay system and Passing-Bablok regression analysis.

Sandwich-based immunoassays are constantly developed for SERS quantification of cardiac biomarkers. For instance, a new SERS-based magnetic immunoassay was designed by Hu et al., which combined magnetic beads and Raman reported embedded Au-core Ag-shell nanotags for sensitive and selective determination of cTnI [64]. In this system, the Raman embedded core-shell nanotags were introduced to increase the stability and sensitivity of the SERS sensor, while magnetic beads ensured the magnetic separation and concentration. Specific recognition of cTnI was accomplished by modifying both SERS tags and magnetic beads with antibodies against cTnI. Once the sandwich-type was formed based on an immune reaction, it was magnetically separated and subjected to SERS analysis using a portable Raman instrument. The developed immunoassay achieved a LOD of 9.80 pg mL^{-1}. 50 serum samples from AMI patients were analyzed using the SERS assay and the FDA-approved clinical chemiluminescence immunoassay (CLIA) to assess the clinical performance of the proposed sensor and its diagnostic potential. The two approaches had a strong correlation, demonstrating the practical usability of the SERS-based immunoassay. This kind of immunoassay was also demonstrated by the same group of authors for selective, sensitive, accurate simultaneous determination of cTnI and heart type fatty acid-binding protein (H-FABP) [65]. The obtained LOD was 0.6396 and 0.0044 ng mL^{-1} for H-FABP and cTnI, respectively, which is much lower than the clinical cutoff value for the diagnosis of acute myocardial infarction disease. Moreover, the described approach allowed simultaneous determination of H-FABP and cTnI in human serum samples, demonstrating great potential for clinical applicability. High recovery factors in the range of 96.4–110.0% were obtained, indicating the accuracy of the method. However, cTnI and H-FABP were spiked in already diluted serum samples of healthy people. Results remain to be confirmed in undiluted samples collected from AMI patients.

Atomically flat Au nanoplates present great potential as sensing nanoplatforms as Lee et al. exploited such substrates to design an innovative sandwich-based approach for SERS detection of cTnI at the attomolar level [66]. In this strategy, AuNPs conjugated with a cTnI aptamer modified with a Raman reporter molecule served as a SERS detection probe, while the aptamer conjugated Au nanoplates enabled the specific capture of cTnI. The detection of cTnI was accomplished by measuring the SERS signal of the AuNPs-on-nanoplate architecture formed upon the specific capture of cTnI. By optimizing the immobilization of the aptamer onto Au nanoplate the binding capacity for cTnI was significantly improved. Therefore, the LOD was determined to be 100 aM (2.4 fg mL^{-1}) in buffer solution and 100 fM (2.4 pg m^{-1}) in serum samples, respectively, which is much lower than the existing cutoff values. Nine clinical samples from both healthy humans and AMI patients were collected and analyzed in parallel using the developed SERS assay and ELISA. Remarkably, the accuracy of the proposed strategy for cTnI detection is higher than that of the conventional ELISA.

A microcavity-based sandwich immunosensor was designed by Wang et al., who combined the light confinement effect of polystyrene (PS) microcavities and the localized surface plasmon resonance (LSPR) properties of AuNPs to achieve simultaneous ultrasensitive SERS quantification of cTnI and CK-MB [67]. The sensor is composed of PS microspheres modified with AuNPs deposited on a silicon wafer as a capture substrate, and Raman-encoded AuNPs as SERS signal probes, respectively. For recognition of cTnI and CK-MB, both SERS tags and the capture substrate were modified with antibodies specific to cTnI and CK-MB. Sensitive and selective detection of cTnI and CK-MB was accomplished by SERS measurement based on a sandwich strategy, reaching a LOD of 3.16 pg mL^{-1} and 4.27 pg mL^{-1} for cTnI and CKMB, respectively. The performance of the method was evaluated in whole blood samples. The obtained recovery factors of cTnI and CK-MB ranged from 94.9 % to 121.6 % while the average coefficient of variance (CV (%)) between replicates was below 15 %, all of these indicating a good accuracy, reproducibility and stability of the developed SERS immunoassay.

Preprints (www.preprints.org) | NOT PEER-REVIEWED | Posted: 12 May 2023 doi:10.20944/preprints202305.0924.v1

In summary, the recent studies concerning SERS-based detection of cardiac biomarkers were focused on sensitivity, selectivity, accuracy, rapidity and portability, with most sensors achieving comparable or superior performance to existing analytical methods in terms of sensitivity and rapidity. While the above described detection approaches picture a rich toolbox available to a scientist wishing to develop new methods for CVD biomarkers detection, many studies are at a preliminary level. Further work is necessary to bring these sensors closer to application, to characterize and validate them fully and to apply them on larger sets of clinical samples in order to prove their utility. Increased application of chemometrics and the use of machine learning/ AI to interpret the complex SERS spectra and extract the specific information pertaining to CVD biomarkers can substantially and rapidly improve the performance of SERS-based detection methods. Aptamers and MIPs appear still underrepresented among the specific receptors used in cardiac biosensors based on SERS. Considering the effervescent research in the field of aptasensors and MIPs for cardiac biomarkers with improved stability and high specificity and reproducibility compared to antibodies, it is anticipated the number of detection strategies based on the combination of these receptors with SERS will significantly grow in the future.

3.3. Fluorescence Based Biosensors

Fluorescence is a preferred detection mode in biomarker analysis, enabling high sensitivity and multiplexing as probes labeled with various fluorescent dyes or nanomaterials become increasingly available and diversified. Examples of fluorescent probes employed in CVDs biomarker detection include fluorochrome dyes and nanomaterials such as lanthanide-doped upconversion nanoparticles (UCNPs) [68], quantum dots (QDs) [69] , carbon dots (CDs) [70], europium chelate-contained silica nanoparticle (EuSiNP) [71], metal organic frameworks, MOFs, [72] etc. These probes were linked to antibodies [68], aptamers [73] or molecular imprinted polymers (MIPs) [74].

Fluorophore-marked bioreceptors were used in both homogenous and heterogeneous systems (Table 1), selectively binding the analyte and thus enabling to correlate its concentration with the fluorescence signal.

Table 1. Performances of recent fluorescence-based methods for the detection of CVD biomarkers.

Method details	**Excitation /emmission wavelength (nm)**	**Analyte**	**LOD (ng/mL)**	LR (ng/mL)	**Selectivity study**	**Analysis of real samples (number of samples)**	**Reference**
LFIA; NaYF4: 30%Yb, 2%Er @NaLuF4 core-shell UCNPs	980/546	Myo	0.21	0.5-400 (DR)	CRP,BSA, NaCl, procalcitonin, hemolysis, high-bilirubin, high-cholesterol plasma	Clinical samples (plasma)	[68]
Aptamer based homogeneous assay; fluorescein	495/517.6	Myo	0.020	0.050 -100	CD63, BSA, EpCAM, and VEGF	Spiked human urine,saliva, serum	[70]
Pyrene-labeled aptamer; homogeneous assay	275/376	Myo	0.068	0.098-7.86	AFP, I, BSA, cTnI, IgA, and IgG	Spiked human sera	[75]

Preprints (www.preprints.org) | NOT PEER-REVIEWED | Posted: 12 May 2023 doi:10.20944/preprints202305.0924.v1

Quantum dot beads@SiO2-COOH (QBs@SiO2-COOH) nanobeads; lateral-flow immunoassay	365/620	CK-MB Myo cTnI	0.25 0.54 0.036	1.5-192 5-640 1-128	-	Human serum	[69]
LFIA, Time-resolved FRET; Donor: polystyrene raspberry nanoparticles coated with europium chelate modified silica nanoparticles; Acceptor: Au nanorods	340/615	cTnI	0.024 (PBS) 0.097 (Serum)	0.02-2 (PBS) 0.15-1.16 (serum)	-	Human serum	[71]
FRET carboxyfluorescein-modified aptamer; homogeneous assay	495/519	BNP	$4.5 \cdot 10^{-5}$	$7.4 \cdot 10^{-5}$-$5.6 \cdot 10^{-4}$	NT-proBNP, CRP,Myo, cTnI IFN, Cys, Gly, HSA, BSA, Arg, His	Blood	[73]
Homogeneous assay Fluorescein-tagged MIP	490	Myo	0.06	$0.06\text{-}6 \cdot 10^{6}$	-	Spiked fetal calf serum	[74]
FRET; Aptamer based homogeneous assay; CdSe/ZnS QD	375/655	CRP	0.045	0.05-1138	Transferrin, thrombin, TNF-alpha, albumin	Spiked and unspiked human serum	[76]
Cu-MOF with nanozyme activity and induced fluorescence upon reaction with H_2O_2; RNA based homogeneous assay; dual fluorescence and colorimetry assay	320/410	CRP	0.24 (C) 0.04 (F)	0.5-50 (C) 0.1-50 (F)	glucose, glutathione, ascorbic acid, iron, creatinine, albumin, calcium	Spiked serum	[72]
Ab-based homogeneous assay; porous hydrogel with encapsulated photonic crystals (PhCs) barcodes; Cy-3 labeled antibodies	Not specified	cTnI BNP Myo	0.009 $8.4 \cdot 10^{-5}$ 0.68	$1x10^{-2}$-$1x10^{3}$ $1 \cdot 10^{-4}$-10 $1\text{-}1x10^{4}$	Mix of BNP and Myo (for cTnI) Mix of cTnI and Myo(for BNP) Mix of cTnI and BNP (for Myo)	Serum	[77]
Aptamer-based lateral flow assay; fluorescent microspheres	470/530	CK-MB	0.63	5-2x103	cTnI, MB	Spiked serum	[78]
LFIA; Bodipy 650 labeled fluorescent latex microspheres; multiplex	Not specified	CK-MB, cTnI Myo	2 0.001 0.01	Not specified	cTnI	Serum samples from AMI patients	[79]

assay for 8 biomarkers from which CK-MB, cTnI and Myo by fluorescence; TC, TG, HDL-C, and UA by dry-chemistry; LDL-C is calculated							
MIP conjugated to CdTe QDs; imprinted hydroxyethylcellulose membrane	635/655	Myo	$3.08x10^{-3}$	$7.39x10^{-3}$–$291x10^{-3}$	cTnT, creatinine, and HSA do not interfere at 10x higher concentrations than Myo	-	[80]
Homogeneous assay; dabcyl -modified aptamer and fluorescently (6-FAM) labeled cDNA;	495/517	Myo	0.07	0.1–5	BSA, AFP, IgA, IgG, HSA, and cTnI	Spiked human serum	[81]

LFIA: lateral flow immunoassay.UCNP: up-conversion nanoparticles. FRET: fluorescence resonance energy transfer. 6-FAM: 6-carboxyfluorescein). cDNA: complementary DNA. Dabcyl : (E)-4-((4-(dimethylamino) phenyl) diazenyl)benzoic acid. TC: cholesterol. TG: triglyceride. HDL-C: high density lipoprotein cholesterol. UA: uric acid. LDL-C: low-density lipoprotein cholesterol.HSA: human serum albumin. AFP: alpha fetoprotein. Ig: immunoglobulin.

Among the various types of tests for the fluorescence -based detection of CVDs, lateral flow assays (LFAs) were a preferred choice and appear particularly promising and when designing as they facilitate simple, rapid, low cost, portable and user-friendly tests [68].

In one example, troponin I detection was achieved by time-resolved fluorescence resonance energy transfer (TR-FRET) using raspberry-type polystyrene microparticles coated with europium chelate-modified silica nanoparticles (EuSiNP) as donor and gold nanorods (GNR) as fluorescence acceptor [71]. The use of a fusion 5 membrane (a proprietary, commercially available porous and hydrophilic membrane) enabled a simplified lateral flow assay system lacking the sample, conjugate and absorbent pads needed with conventional strips made of nitrocellulose. The test was conceived as a competitive immunoassay whose sensitivity was enhanced thanks to TRF measurements, enabling to remove the background fluorescence by taking advantage also of the long fluorescence decay time of lanthanides. The lateral flow strip has a test line consisting of cTnI conjugated Eu-raspberry particle and a control line with immobilized anti-mouse-antibody-conjugated Eu-raspberry particle (Figure 5). The quencher particles, GNR conjugated with a specific antibody for cTnI Ab are first mixed with the sample. When placed on the designed sample zone of the strip they advance through capillary force towards the test and control lines. In the absence of cTnI in the sample, the GNR-cTnIAb particles bind to the cTni-EuSiNP particles in the test line, drastically decreasing their fluorescence signal. The excess quencher particles are captured at the control line. In the presence of cTnI, the GNR-cTnI Ab bind to the biomarker in the sample instead of the cTnI at the test line, thus the quenching of the fluorescence signal at the test line is reduced (i.e, the fluorescence is higher). The competitive test was conducted both in buffer and serum samples, featuring LODs of 24 pg/mL and 97 pg/mL, respectively. This LFIA system was compared with standard cTnI ELISA assay and showed good accuracy.

Preprints (www.preprints.org) | NOT PEER-REVIEWED | Posted: 12 May 2023 doi:10.20944/preprints202305.0924.v1

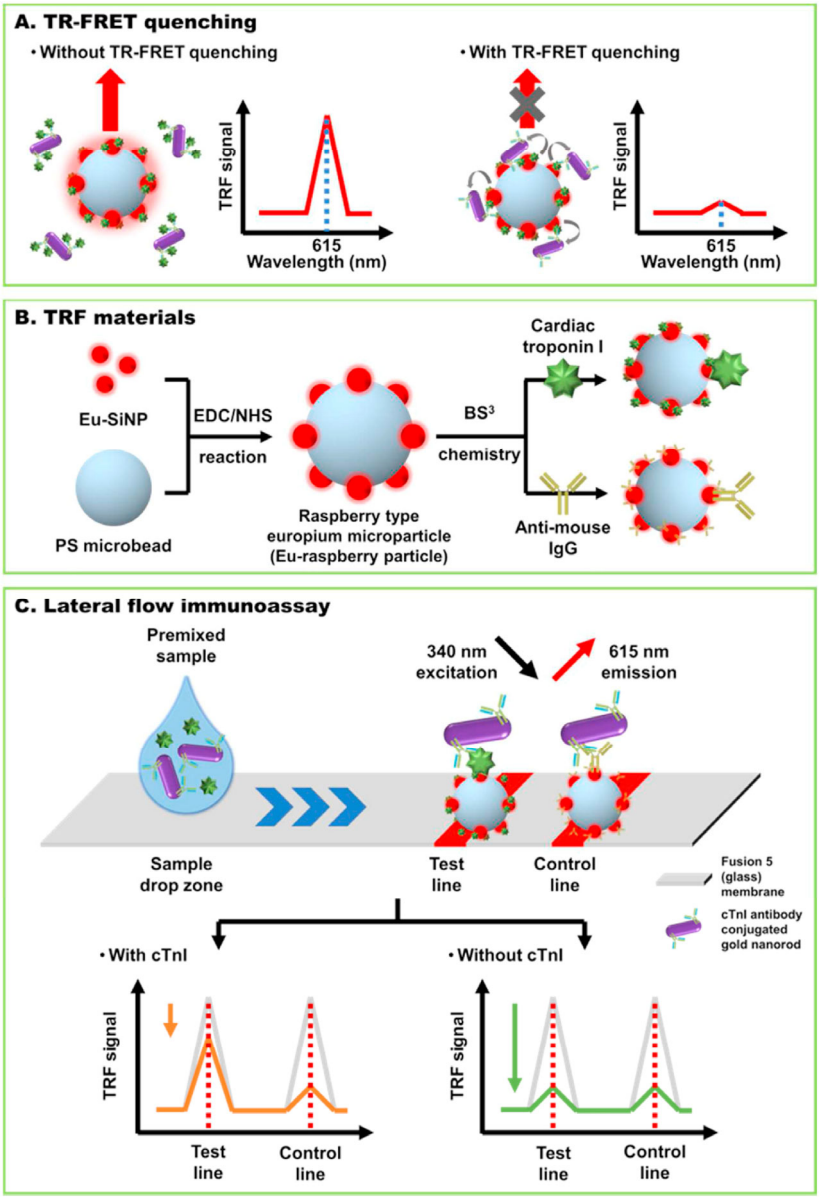

Figure 5. Principle of the TR-FRET LFIA for cTnI. A: Fluorescence quenching mechanism by TR-FRET using Eu-SiNP and GNR. B: The synthesis of the donor raspberry type Eu-SiNP.C: The competitive assay used in the LFIA: cTnI in the sample competes with cTni anchored on the Eu-SiNPs at the test line for binding to the cTnI Ab-GNR conjugates. Thus, in the presence of cTnI the fluorescence at the test line is high. In the absence of the biomarker, the binding of the cTnI Ab-GNR conjugates to the cTni / Eu-SiNPs drastically quench the signal at the test line. Reproduced from [71] with permission from Elsevier.

The traditional bench-top detection equipment for fluorescence measurements is bulky and expensive. Portable readers facilitate the adoption of fluorescence methods by users and fully exploite the potential of LFIA systems for POC measurements. A POC platform including a portable detection module and a sample processing module (LFA strip) relied on upconversion nanoparticles (UCNPs) for myoglobin detection [68]. The UCNPs were NaYF4:Yb,Er@NaLuF4 core-shell nanoparticles and the specificity of the detection was ensured by a classic sandwich immunoassay. The ratiometric approach, where the concentration of myoglobin was proportional to the fluorescence intensity ratio of test and control (T/C) lines helped minimizing the sensitivity of the assay to possible deviations between different strips. A 10-minute period was optimum for the immune-reaction to take place so the T/C ratio reached saturation. The test is rapid, the time per assay being three times shorter than

Preprints (www.preprints.org) | NOT PEER-REVIEWED | Posted: 12 May 2023 doi:10.20944/preprints202305.0924.v1

for the standard method. Interestingly, different types of plasma sample (hemolysis, high-bilirubin, high-lipids) were analyzed to test potential interfering effects. Based on recoveries of 89.0-110.5% from spiked samples and CVs of less than 10% the authors concluded that the type of sample had little effect on the test result. The results obtained with this LFIA method were compared to the Abbott Chemiluminescence assay, typically used in the clinical practice, showing great consistence between them (i.e., coefficient of determination of 0.95, slope of the linear regression =0.92). Intra and inter-assays performed with LFIA were characterized by coefficients of variation (CVs) under 14 %. showing the good precision of the proposed sensor strip.

Molecularly imprinted polymers are increasingly researched as antibody replacers in the aim to decrease costs and improve the stability and reproducibility of bioanalytical testing devices. Moreover, significant advances have been made with regards to such "plastic antibodies" with high affinity and specificity for high molecular weight molecules including protein biomarkers. Due to their large surface displaying a variety of functional groups developing MIPs with cavities complementary to such large target molecules is a very difficult task.

A MIP-based fluorimetric assay was developed to detect myoglobin in biological samples [74]. The MIP was obtained from fluorescein *O*-acrylate and was used to capture myoglobin from test samples in a homogeneous assay. To ensure that the measured fluorescence signal was due exclusively to the myoglobin- bound MIP, supermagnetic iron oxide nanoparticles (SPIONs) functionalized with myoglobin were added to the sample vial, after the MIP-sample binding reached saturation (5-10 minutes). The SPION particles were used to remove by using a magnet the excess, unbound MIP so that only the target protein-bound MIPs was left in suspension in the vial and the fluorescence signal was proportional to the quantity of myoglobin in the sample (Figure 6). Noteworthy, the magnetic nanoparticles were obtained by a "green" synthesis method. The logarithm of the fluorescence intensity varied linearly with the logarithm of protein concentration in the range from 60 pg/mL to 6 mg/mL. The imprinting factor of the MIP is 1.95 and the non-specific binding, evaluated with BSA, amounted to 42.4%, about half of the response for the same concentration of myoglobin (3mg/mL). In the same time, when analyzing spiked fetal calf serum samples spiked with myoglobin, the average recovery was 93 %, indicating that the technique has adequate accuracy for myoglobin detection in biological samples. Together this data shows a good potential for analyzing clinical samples but also the necessity to include control tests with non-imprinted polymer (NIP) particles in order to account for the non-specific effects. A wider interference study is necessary to prove the selectivity of the assay. By improving the imprinting factor and preventing non-specific adsorption effects, the performances of the assay can be enhanced further.

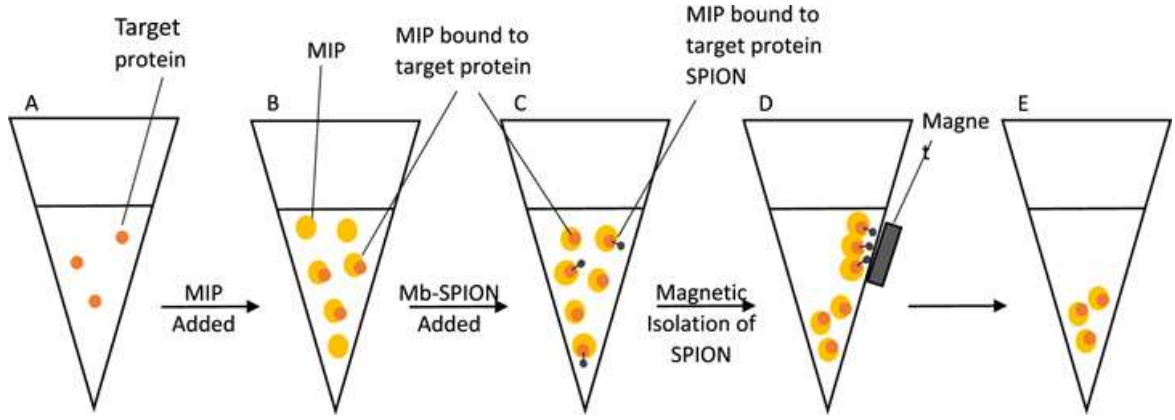

Figure 6. Principle of the MIP-based fluorimetric homogeneous assay for myoglobin. The fluorescein-tagged MIP is incunated with the sample and binds myoglobin. Next, myoglobin-functionalised SPION paericles are added to bind the excess MIP. The SPION particles and conjugates with MIPs are removed via a magnet. The fluorescence due to the remaining MIP particles is measured and correlated with the concentration of myoglobin in the sample. Reproduced from [74] with permission from the authors.

 doi:10.20944/preprints202305.0924.v1

An alternative to starting from a fluorophore-labeled monomer for obtaining the MIP is to label the MIP with fluorescence producing probes. e.g., with quantum dots (QD, [80]). A MIP-imprinted hydroxyethylcellulose membrane where the MIP was tagged with CdTe QD was used for the detection of myoglobin starting from 7.39 pg/mL (the lower limit of the linear range). The imprinted strip had a storage stability of (at least) 15 days. The detection was achieved in human serum that was diluted 1000 times with buffer. The interference study has shown that cardiac troponin T, creatinine, and human serum albumin do not significantly affect the sensor's response when tested at concentrations ten times higher than the level of myoglobin. Nonetheless, some proteins, e.g., human serum albumin in present in much higher excess compared to myoglobin. Testing a "standard" panel of potentially interfering compounds at ratios reflecting those typical for clinical samples would be a big step forward to enable an objective evaluation of this and all other various sensing concepts proposed.

The challenges associated with measurements in complex samples such as serum are not trivial, as proven in another report on the detection of myoglobin [81]. The test relies on the conjugation of a dabcyl-labeled aptamer with a FAM-labeled partially complementary DNA sequence, resulting in the quenching of the FAM fluorescence signal in the absence of myoglobin and its specific recovery in the presence of myoglobin. The authors noted that proteins that are present in serum in high concentration, such as human serum albumin, present at 35-50 mg/mL, induce a high fluorescence background. For accurate measurements of cTnI the sample pretreatment consisted in diluting the serum by a factor of 10, and further purification by filtration through a 30 kDa cutoff centrifuge filter.

In the recent period the trends of developing multiplexed assays and assays based on dual detection modes continued. With regards to the latter, an illustrative example is a biosensor for the measurement of CRP by both colorimetry and fluorescence [72]. At the core of the assay stands a Cu-MOF material coated with an RNA aptamer specific for CRP. The Cu-MOF has peroxidase like activity, functioning as catalyst for the classic reaction of TMB and H_2O_2 resulting in the blue colored compound measurable by colorimetry. The Cu-MOF also presents "stimulated fluorescence", i.e., is not a fluorescent material per se but it is converted into one, following its reaction with H_2O_2; then, if excited at 320 nm it will emit at 410 nm. The catalytic activity and the stimulated fluorescence properties of the Cu-MOF are both inhibited when the material is coated with the aptamer and recovered when the aptamer is desorbed following its interaction with the CRP in the sample. The approach enables to have two reliable results (by fluorescence and colorimetry) with one platform (Figure 7). The size of Cu-MOF particles is in the sub-micrometer to micrometer range as characterized by FESEM. A selectivity study was conducted for both detection techniques and concluded that the signal for CRP was high and selective when compared to several compounds tested with 100 times more concentrated solutions than CRP. Nonetheless, in real serum fluid the quantity of some biomolecules such as serum albumin are more elevated than the tested amounts. Further investigations are thus necessary and they need to include other cardiac biomarkers as potential interferents in order to definitively prove that the analytical system is adequate as a diagnosis tool. When the method was applied on spiked diluted serum, the recovery percentages were 84-102 %, showing good accuracy for real sample testing. Unfortunately, the analysis of a set of clinical samples and the comparison with a standard method toward comparing the obtained data was not addressed and remains as a next step for advancing the proposed concept.

Preprints (www.preprints.org) | NOT PEER-REVIEWED | Posted: 12 May 2023 doi:10.20944/preprints202305.0924.v1

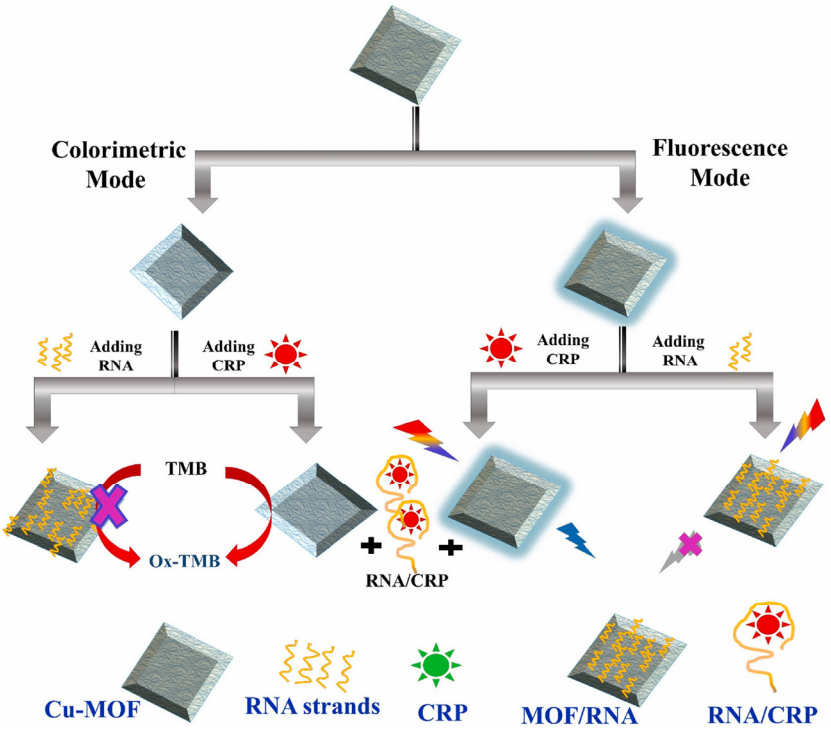

Figure 7. Principle of the detection of CRP by the dual colorimetry-fluorescence method relying on Cu-MOF and RNA-aptamer. Details are given in the text. Reproduced from [72] with permission from Elsevier.

The multiplexed detection of 8 biomarkers with a single strip was demonstrated by Huang et al [79], which combined the analysis of Myo, CK-MB, and cTnI by a fluorescence sandwich immunoassay with the determination of cholesterol (TC), triglyceride (TG), high density lipoprotein cholesterol (HDL-C) and uric acid by dry chemistry. Additionally, the content of low-density lipoprotein cholesterol (LDL-C) in the sample was derived by calculation. The strip was intended as a diagnostic tool for acute myocardial infarction (AMI). Towards this goal, the selectivity for cTnI detection was first proven by comparing the signals for cTnI (50 ng $mL^{-1)}$ with those for CK-MB (500 ng mL^{-1}), Myo (500 ng mL^{-1}), TC (50 mmol L^{-1}), TG(50 mmol L^{-1}), UA (50 mmol L^{-1}), and HDL-C (50 mmol L^{-1}) . The analytical performances of the strip feature among others detection limits for Myo, CK-MB and cTnI of 10 pg /mL, 2pg/mL and 1 pg/mL, respectively. Following detailed characterization, the sensor strip was used to analyze a set of serum samples collected from AMI patients and the results were compared with the current clinical methods based on chemiluminescence immunoassay (CLIA). The good correlation between the two sets of results stands as evidence of the applicability and usefulness of the proposed 8-in 1 test.

In the search to enhance the sensitivity of the measurements and reduce the time per assay, new materials are critical. CdSe/ZnS quantum dots of 14 nm medium size were assembled into nanobeads by encapsulation in CTAB and were subsequently coated with SiO_2 and polyvinylpyrrolidone in order to preserve their luminescence properties in various environmental conditions [69]. The coated beads (QBs@SiO2-COOH)with an average diameter of 235 nm displayed an enhancement of 1967 times in luminescence and a remarkable stability in complex samples and at different pH and temperatures [69]. The principle of the test is that classic for a LFIA, where the ratio between the fluorescence signal at the test and control lines are proportional to the biomarker concentration in the sample (Figure 8).

Preprints (www.preprints.org) | NOT PEER-REVIEWED | Posted: 12 May 2023 doi:10.20944/preprints202305.0924.v1

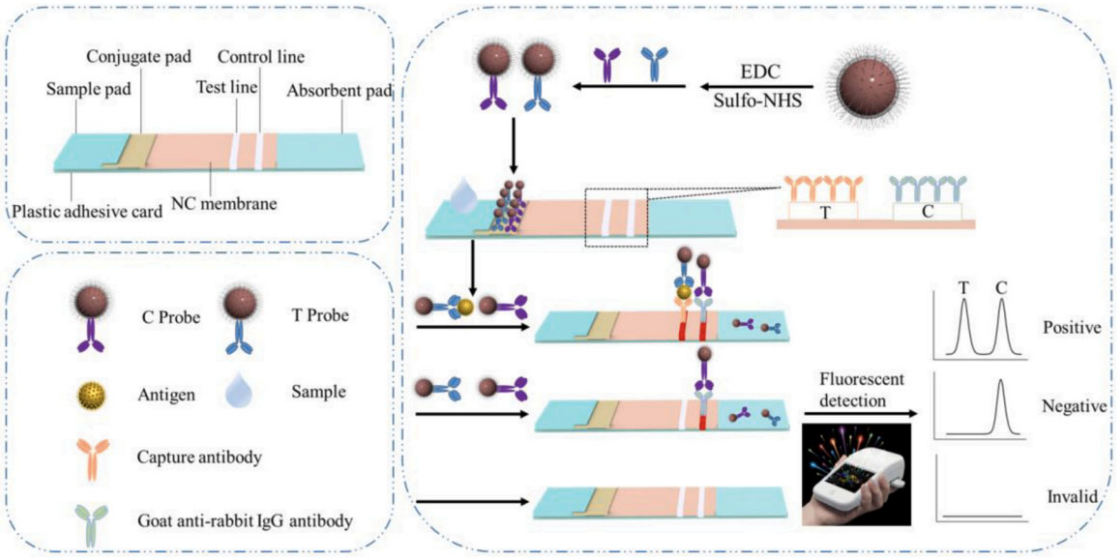

Figure 8. Principle of the QBs@SiO2-COOH-based LFIA and of the detection of cTnI. Reproduced from Li et al, 2021 [69] with permission from Elsevier.

Nonetheless, the strong luminescence and optimized ratio between the nanobeads and the cTnI antibodies were the key to achieve a detection limit of 0.036 ng mL-1, i.e., about 20 times lower than the smallest concentration detectable by a similar LFIA using SiO2-coated QDs. The stability of the sensor strips was evaluated based on the measurements for four concentrations of cTnI and the results support the stability of the strip stored at either room temperature, 37º C or 45º C for 120 days. By appropriate modification with specific antibodies, the sensor was used for the simultaneous measurement of CK MB, Myo and cTnI. Remarkably, a set of 38 human serum samples were analyzed in parallel with the proposed QBs@SiO2-COOH-based LFIA and by ELISA and it was determined that the concentrations of cTnI, CK-MB and Myo measured by the two methods were linearly correlated, with slopes of the fitting lines very close to 1 and correlation coefficients R =0.980-0.991. The assay time with this strip was 10 minutes and the reproducibility of the test was adequate, i.e., the CV of intraassay and inter-assay tested at 3 concentration levels of cTnI were below 8 %. Noteworthy, a large set of 103 clinical serum samples were analyzed for their level of cTnI in parallel by the LFIA and by a standard chemiluminescence method and the results were in good agreement, supporting the accuracy of the LFIA. This work is a very nice illustration of a detailed, very informative research reporting on all of stability characteristics, analytical performances, feasibility for testing clinical samples and comparison with standard methods. The benefits of the new nanobeads material are clear as they are quantitatively evaluated in comparison with the starting, simple QDs (in terms of luminescence intensity and detection limit achieved for cTnI). This work serves as a model for studies aiming to close the gap between research laboratory and clinical practice.

In summary, fluorescence enables a high flexibility in designing the detection approach due to the variety of fluorochrome probes and dyes with unique properties. Fast simplified POC detection enabled by portable readers combined with LFA appear as the main avenue of research and vector of progress towards commercially available devices. Some of the recent studies focus on new materials and specific receptors for achieving a large linear range and great sensitivity. The search for ultrasensitivity of detection was prompted in the recent works by the desire to depart from the traditional approaches based on invasive blood testing towards patient-friendlier procedures, e.g testing of saliva [70] or analysis from very low volumes of blood. Thus, efficient signal amplification was ensured e.g by deoxyribonuclease I-aided target recycling (Chen, RSC Advances 2019) and in some of these works issues like selectivity, real sample testing and verifying the accuracy with standard assays remain to be addressed. A glimpse at the data in Table 1 emphasizes that in many cases the verification of accuracy was limited to spiking and recovery studies. Not all concepts were

 doi:10.20944/preprints202305.0924.v1

verified with clinical samples and compared to standard or current methods in clinical laboratories. While the main reason for switching from antibodies to MIP is to gain in stability, this aspect was rarely investigated in detail, for long time periods. Despite the progress in the biomarkers analysis, there are significant challenges related to the complex composition of the serum samples that new assays relying on new materials and recognition mechanism must overcome. Works reporting validation tests and the analysis of large sets of clinical samples, multiplexed detection for analyzing specific CVDs and combining different detection modes in the same analytical platform converge with studies on new materials and hint to a promising future of fluorescence-based tests for the CVD biomarkers.

3.4. Chemiluminiscence and Electrochemiluminescnce-Based Biosensors

Chemiluminescence (emission of light induced by a chemical reaction) and electrochemiluminescence (ECL, where the luminescence is triggered by chemical species formed in an electrochemical reaction) facilitate the extremely sensitive detection of various analytes.

For example a chemiluminescence assay for cTnI requiring 5 μL of serum sample relied on a microfluidic chip and magnetic beads modified with aptamer for the specific capture of the protein biomarker [82]. The captured cTnI was bound to a primary antibody that was further linked to a HRP-labeled. anti-IgG antibody. The signal was due to a chemiluminescent HRP substrate and was varied linearly with cTnI concentration in the range from 196 to 3931 ng/L. The accuracy of the assay was proven by recoveries of 90-108.5 % from spiked serum samples and by the similarity of results (ie. within 1.14-7.57%) with standard chemiluminescence immunoassay performed with the commercial Siemens ADVIA Centaur systems for five human serum samples containing between 16.3 and 927.3 ng/L cTnI. Remarkably, the microfluidic chip-based platform enabled the analysis of 6 samples in 30 minutes.

Multiplexed, shorter analysis of cTnI, CK-MB, and Myo (within 17 minutes) was achieved with another microfluidific platform with chemiluminescence detection [83]. In a classical manner, the specificity of the detection was ensured via an antibody-based sandwich while the chemiluminescence was produced in a reaction catalyzed by HRP, used as label for the detection antibodies. Nonetheless, mixing the detection antibodies with the sample upon introducing it into the microfluidic chip enabled to shorten the assay time compared to ELISA. Obtaining the chip by 3D printing was reported to reduce the costs.

An ECL assay was developed by [84] for the detection of NT-proBNP down to a detection limit of 0.11 pg/mL and a linear range between 0.25 pg/mL and 100 ng/mL. The signal generation was based on the electrochemiluminescence-resonance energy transfer between gold nanoparticles modified with silver nanocubes and a metal-organic framework of type MIL-125. The strategy for obtaining the donor luminophore by coating silver nanocubes (AgNCs) with semicarbazide and attaching them to Au nanoparticles resulted in a stable ECL signal with a three times higher intensity compared to that provided by AgNCs alone. The modified particles were deposited on an electrode and a primary antibody specific to NT-proBNP was attached to the donor luminophore. The Ti(IV) based metallic organic framework MIL-125 having an adsorption spectrum overlapping with the emission spectrum of the donor, quenched the luminescence of the donor. Thus when NT-proBNT was sandwiched between primary and secondary antibodies fixed on the donor and acceptor particles, respectively, the decrease in ECL was directly correlated with the concentration of the cardiac biomarker in the sample. The approach led to similar results as classic ELISA and the accuracy was moreover proved by the good recovery (96.8% -100.2%) in experiments with human serum spiked at three concentration levels.

While used in standard clinical laboratory equipment these detection methods were less represented in the biosensors field compared to e.g., fluorescence, unravelling great sensor development opportunities for the near future.

Preprints (www.preprints.org) | NOT PEER-REVIEWED | Posted: 12 May 2023 doi:10.20944/preprints202305.0924.v1

3.5. Colorimetry-Based Biosensors

Colorimetry is a simple optical method which measures the color change when modifications occur as the result of a reaction in solution [85] or on a surface (e.g lateral-flow assay. Colorimetry is very promising in developing point-of-care (POC) testing because it can be rapid, cheap and can be carried out by unskilled personnel.

Consequently, several studies in the recent years used this detection method for the analysis of CVD biomarkers. Data summarized in Table 2 shows a variety of colorimetry-based approaches aimed at sensitive and accurate detection meeting the clinical cutoff for specific CVD biomarkers in serum samples.

Table 2. Performances of some colorimetry-based approaches for the detection of CVD biomarkers.

Method details	Assay time	Analyte	LOD (ng/mL)	LR (ng/mL)	Selectivity study	Analysis of real samples (number of samples)	Reference
AuNP/Apt;salt-induced aggregation of AuNPs	5 min	CER	$1.2 \cdot 10^3$	8.89×10^2–2.0×10^4	BSA, aprotinin, proteinase K, L-glutamine, urea, ascorbic acid. BSA interferes at > 100 nM	Spiked diluted human urine	[86]
Enzyme-free immunosorbent assay; Au nanovesicles with integrated allochroic dyes	>81 min	NT-proBNP CK-MB cTnT	$7 \cdot 10^{-2}$ 0.91 $7.8 \cdot 10^{-3}$	0.1 -10^5 1-500 0.01-2	-	Human plasma pectoralgia patients and healthy individuals	[87]
MB)/ capture DNA/Apt/HRP-DNA1/DNA2	>165 min	Myo miRNA-141	8.75	0- 7×10^3	Gox, HAS, BSA, ALP	Spiked human serum	[85]
DNA hydrogel with encapsulated PtNPs/Cu-CPP(Fe); EXPAR combined with CRISPR-CAS14a	>100 min	CK-MB	0.355 pM	3.55×10^{-4} nM–119.03 nM (DR) 5×10^{-4} nM–100 nM (LR)	cTnI, H-FABP, CRP, calcitonin	Spiked human serum samples	[88]
Microfluidic chip with DNA hydrogel with Apt/cDNA and embedded AuNPs	>3h	CK-MB	0.147 (colorimetry at 520 nm, C) 2.4×10^{-3} (by coupling with microfluidic chip and cell phone as	8.7 -$6.53 \cdot 10^4$ (C) 17.4-$4.875 \cdot 10^4$ (M)	cTnI, Myocardial fatty acid binding protein (H-FABP), CRP, calcitonin	Spiked serum	[89]

Preprints (www.preprints.org) | NOT PEER-REVIEWED | Posted: 12 May 2023 doi:10.20944/preprints202305.0924.v1

			readout, M)				
Cu-MOF HRP-like nanozyme/Apt; dual colorimetry and fluorescence detection	>135 min (colorimetry-C) >10h (fluorescence-F)	CRP	0.24 (C) 0.04 (F)	0.5-50 (C) 0.1-50 (F)	glucose, glutathione, ascorbic acid, iron, creatinine, albumin, calcium	Spiked serum	[72]
Microfluidic chip; AB/Ab1/biomarker/Ab2-biotin/streptavidin-HRP	20 min	cTnI hFABP NT-proBNP	$9.56{\cdot}10^{-3}$ $95.5{\cdot}10^{-3}$ $5.29{\cdot}10^{-3}$	QL: $28x10^{-3}$ 0.290 $16.04x \cdot 10^{-3}$	-	Spiked plasma; samples from healthy + patients with ACS, DCM and AS	[90]
Paper microfluidic device; sandwich immunoassay; conjugates of Ab-nanomaterials (AuNPs, AgNPs, Au urchin)	10 min	GPBB CK-MB cTn T	0.5 0.5 0.05	0-100 0-100 0-200	HSA, uric acid, ascorbic acid	Clinical human sera	[91]
LFIA; Ab-AuNPs conjugates	1-1.5 min	MB CRP DDm	30 300 300	30- -$3x10^3$ $3x10^2$ -$3x10^4$ $3x10^2$ -$1x{\cdot}10^5$	no cross reactivity with the other biomarkers	Human serum	[92]
LFIA , AbHRP mimicking nanozyme (Au@Ag-Pt NPs) conjugate	10 min	CRP	$1.5x10^{-2}$ in serum	-	serum albumin,,IgG, procalcitonin, cTnI cTnT	Spiked rabbit serum	[93]
Sandwich assay citicoline-BSA/CRP/Apt-AuNPs (AuNPs as HRP mimicking nanozyme)	≈80 min	CRP	$8x10^{-6}$	0.1 - 200	Myo, cTnI, growth differentiation factor 15, BSA, γ-globulin, non-fat milk powder, aspartic acid, arginine, glycine, glucose, fibrinogen, transferrin.	Rat serum and spiked rat serum	[94]
ELONA (direct and sandwich); SA/biotinin-Apt/ streptavidin-HRP	2.5-3h	cTnT	3.42 nM (direct assay) 3.13 nM (sandwhich)	-	Non-specific adsorption observed for undiluted serum (direct assay)	Human serum	[95]
Microfluidic paper; capture Ab1/cTnI/Ab2/H1/hemin(DNAzyme)	45 min	cTnI	$1x10^{-3}$	0.005 -100	HAS, Hb, CEA, AFP	Spiked serum	[96]

 doi:10.20944/preprints202305.0924.v1

Glass plate/ MOF-818 nanozyme confined in porous WO_3/Apt-Glu/ catechol oxidase-mimic, Exo-I assisted signal amplification	>30 min	cTnI	$1.8x10^{-5}$	$5x10^{-5}$ - 100	CRP, Myo, HAS, IgG, CEA, AFP.	Spiked serum, unspiked serum	[97]

HRP: horseradish peroxides; Apt: aptamer.MB: magnetic beads; Myo: Myoglobin; Gox: glucose oxidase (Gox); HSA, human serum albumin; BSA: bovine serum albumin. ALP: alkaline phosphatase. AB: antibody. hFABP: heart-type fatty acid binding protein. ACS: acute coronary syndrome. DCM: dilated cardiomyopathy. AS: artic stenosis. QL: limit of quantitation. GPBB: glycogen phosphorylase isoenzyme. LFIA: lateral flow immunoassay, Hb: hemoglobin, CEA, carcinoembryonic antigen. AFP: α-1-fetoprotein. ELONA: enzyme-linked oligonucleotide assay. Cu-TCPP(Fe): metallic organic framework with with Fe (III) meso-tetra(4-carboxyphenyl) porphine chloride (TCPP-(Fe) and Cu. PtNPs; Pt nanoparticles.EXPAR:exponential amplification reaction. CRISPR: Clustered regularly interspaced short palindromic repeat.

Paper based, microfluidic chips or solution-based assays were reported (Table 2). Most analytical approaches are derived from sandwich type immunoassays by replacing enzymes with nanozymes [72,93,97] and DNAzymes [96]. This corresponds to a growing trend compared to the previous period, as is the case also with the development of aptamer based assays, which increased in the context of continuing efforts to select new specific sequences with high affinity for CVD biomarkers (e.g for cTnT, [95]. Oligonucleotides enable additional sensing strategies compared to antibodies including new approaches for signal generation and amplification e.g. supersandwiches made by DNA hybridization [85], DNAzymes [96] and Exo -I assisted amplification [97]. Increased stability is the major goal driving these changes from enzymes and antibodies to nanozymes/DNAzymes and aptamers, respectively. From this perspective, the lack of stability data of these new materials and sensors is intriguing and disappointing.

The time per assay ranged from 1.5-20 minutes [86,90-92] indicating potential for POC testing) to more than several hours (Table 2). Undiluted serum was used in several LFIA [92] and homogeneous assays, however in general, dilution with buffer was found to be an adequate procedure to bring the sample concentration in the linear range of the method and minimize interferences.

Screening several CVD biomarkers simultaneously is time-saving and helps establishing the type of CVD. Ozen et al [90]. developed a Total Microfluidics platform for Multiplexed diagnostics (ToMMx) for detection of cardiac troponin-I (cTnI), heart-type fatty acid binding protein (hFABP) and N-terminal pro-brain natriuretic peptide (NT-proBNP) (Figure 9). The assay included similar steps as ELISA, with modifications adapted for ToMMx. The platform is filled iteratively with mineral oil, washing buffer and water-based reagents with the help of surface tension differences so these components did not mix. They were preloaded before sample processing. The magnetic beads employed in the assay are actuated using a magnet. The analytes are specifically captured between Ab immobilized on the beads and a biotinylated secondary Ab, then a complex is formed when adding streptavidin- conjugated poly-HRP. The analytes' concentration is evaluated by color changes when TMB s added as substrate whose oxidation is catalyzed by HRP. A set of clinical samples was analyzed in parallel by the platform and by standard ELISA and the results have shown that the proposed method is precise and accurate. The sample set included 38 pacient samples corresponding to different type of CVDs and 12 control samples. Using the platform's results the pacients were diagnosed with an accuracy of 91 % for acute coronary syndrome (via cTnI and hFABP) and 95% for severe symptomatic aortic stenosis (via NT-proBNP), respectively. When NT-proBNP was used as a diagnostic biomarker, its detection with this analytical platform led to the identification of patients suffering from dilated cardiomyopathy with 100 % accuracy.

Even if these results are very promising, a wide selectivity study is mandatory in order to validate the method. The total time of the assay is less than 20 minutes, that is 15-fold reduced compared with ELISA. In the future, the authors predicted that by integrating ToMMx platform with portable detection systems such as smartphones and by mass production of the assay kit this

Preprints (www.preprints.org) | NOT PEER-REVIEWED | Posted: 12 May 2023 doi:10.20944/preprints202305.0924.v1

multiplex method can become easy and cheap, accessible for everyone. (*Total Microfluidic chip for Multiplexed diagnostics (ToMMx)*)

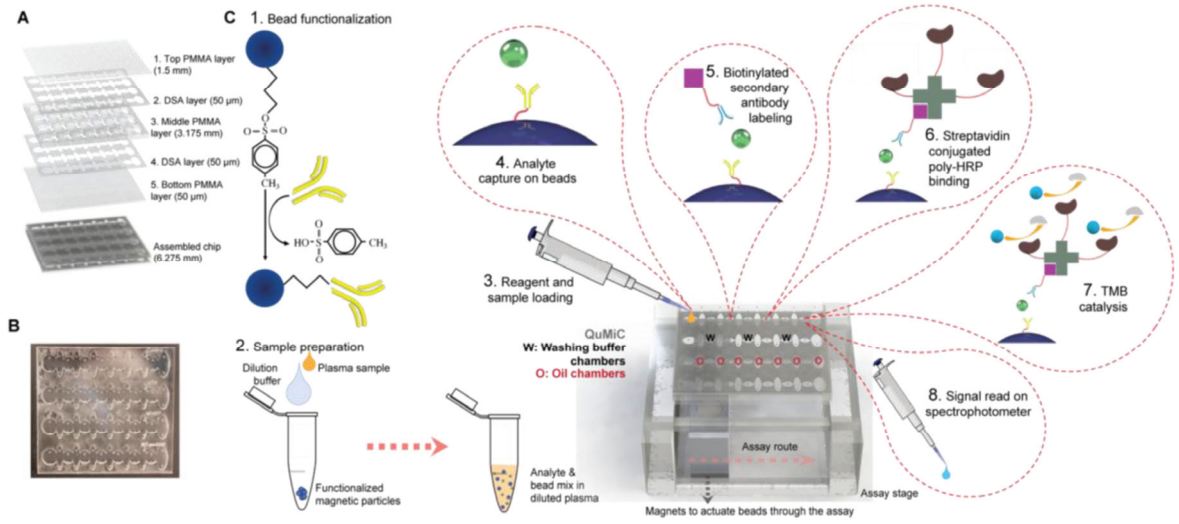

Figure 9. Construction and working principle of the Total Microfluidic chip for Multiplexed diagnostics (ToMMS). **(A)** Polymethyl methacrylate (PMMA) and double-sided adhesive (DSA) polyethylene terephthalate (PET) film layers of ToMMx design. **(B)** Laser-cut and assembled ToMMx. **(C)** Bead functionalization, sample preparation and assay steps of ToMMx. **(1)** Functionalization of tosyl-activated magnetic beads with analyte specific primary antibodies. **(2)** Sample dilution buffer, plasma sample and functionalized beads mixed in tube as sample preparation. **(3)** Assay reagents, buffers and sample loading on ToMMx. **(4)** Analyte in the sample captured on antibody functionalized beads. **(5)** Analyte-antibody complex labeled with biotinylated secondary antibody. **(6)** Streptavidin conjugated poly-HRP binding to antibody-antigen-antibody sandwich complex. **(7)** TMB substrate catalysis by poly-HRP in the complex. **(8)** Evaluation of analyte concentration via color change in the sample after transferring the colored liquid to a 96-well plate, mixing with stop solution and reading in with a spectrophotometer. Reproduced from [90] with permission from Elsevier).

With the same aim of simplified assays for CVD biomarker detection, Wang et al [96] developed an ingenious instrument-free detection method for cTnI where the length of a "coffee ring" type colored band, developed on a microfluidic paper device -simply measurable with a ruler- was proportional with the concentration of the cTnI in the sample. The making of this microfluidic device involved a pair of antibodies (for the sandwich-type sensing) as well as oligonucleotides (to form a DNAzyme) and other reagents: hemin (for the DNAzyme), iodide and H_2O_2 (DNAzyme substrates) and starch (for the blue color development by reaction with iodine). The work nicely illustrates the versatility of DNA hybridization which in this case served to assemble the DNAzyme. Specifically, the detection antibodies were labeled with oligonucleotides that hybridized to complementary DNA to form a G quadruplex. In the presence of hemin this acts as a peroxidase mimic catalyzing the oxidation of iodide to iodine.

In another report, DNA hybridization was used to (i) attach the aptamer to a capture probe fixed on magnetic beads, (ii) assemble the enzyme-labeled signaling probe [85] and (iii) bind the signaling probe to the aptamer. The quantitative test for myoglobin was performed in a test tube and an optical amplifier was used as readout instead of a spectrophotometer to simplify the equipment needed for the quantitative detection. Developed as a turnoff assay, the measurement relied on the proportionality between the decreased amount of HRP-labeled probe hybridized to the aptamer (and consequently, lower color intensity following the enzymatic reaction) and the quantity of myoglobin in the sample, bound by the aptamer. This test required almost 3 hours from which the longest step (90 minutes) was the attachment of the DNA-based, HRP- labeled "supersandwich" signaling probe. Consequently, the time per assay remains an aspect to be significantly improved in the future.

 doi:10.20944/preprints202305.0924.v1

New aptamers were recently selected for cTnI [95], targeting different epitopes of the biomarker and with affinities of KD = 122 ± 14 nM (Apt.1) and 190 ± 20 nM (Apt2). These were used to developed an Enzyme Linked Oligonucleotide Assay (ELONA). The work emphasized one important advantage of the sandwich over the direct detection format, namely it enabled to mitigate the matrix effects and observe the same sensitivity when analyzing cTnI in undiluted serum as in the buffer solution.

Aiming to replace enzymatic labels to increase the stability and reduce costs, while allowing for multiplexed colorimetric sensing, Pu et al [87] reported the use of phenolphthalein, methyl red, bromothymol blue dyes as labels enabling the specific, simultaneous immunoassay of 3 biomarkers for AMI (NT-proBNP, CK-MB and cTnT). The dyes with pH dependent color were loaded on Au nanovesicles and their loading/release was temperature- controlled. The nanovesicles were functionalized with specific antibodies and the assay was performed similarly to a classic ELISA. A comparative analysis of a set of serum samples via the proposed test and by a standard immunofluorescence assay typically used in a clinical laboratory indicated similar results. The new assay has the benefits of higher sensitivity and wider linear range.

Xie et al [94] described an antibody free, ELISA like assay for CRP where the biomarker was sandwiched between a conjugate of citicoline and BSA as capture probe and an aptamer as detection probe. The aptamer was labeled with AuNPs acting as HRP-mimicking nanozyme while TMB was used as nanozyme's substrate. Remarkably, the reproducibility of the materials used in the test, i.e. the citicoline-BSA conjugate and the AuNPs labeled aptamer was assessed by performing the analysis of a serum sample with 5 lots. Low, acceptable variations between batches of materials were found as indicated by the CV of 7.11% for the CRP concentration in the sample. The accuracy of the test was demonstrated by the similarity of results obtained by the proposed assay and classic ELISA, performed in parallel.

While noble metals were increasingly used as colorimetric probes and as nanozyme labels the kit developers authors struggled to minimize the amounts of these expensive and rare materials [93]. For example, Panferov et al [93] integrated trimetallic nanoparticles made from Au, Ag and Pt into a lateral flow immunoassay (LFIA) for C-reactive protein (CRP) where Pt atoms were dispersed on the surface of nanoparticles rather than forming a full coating. With this nanozyme, the detection limit was improved to 15 pg/ml CRP, i.e., 65 times compared to using AuNPs alone while the ratio material/catalytic performance was minimized. It is also important to mention the same authors' preoccupation towards less invasive approaches as besides testing serum sample, the researchers did some preliminary studies with capillary blood. While acknowledging that the background interference found for some samples impose the necessity of sample pre-treatment, the problem might find an easy solution in the future and the use of capillary blood appears as an avenue worth investigating. In view of the adoption as a POC device, the assay will benefit from further simplification to eliminate the need that the enzymatic substrate, 3,3, diaminobenzidine and the H_2O_2 be added separately. Nonetheless, the measurements with the described LFIA were performed in less than 10 minutes.

A very recent report combining aptasensing with nanozymes for the detection of cTnI [97] included several innovative aspects. For increased efficiency, the nanozyme catalyzed reaction was confined into pores of tungsten trioxide (p-WO3) serving as reactors. The color-producing signal readout was based on "enzymatic" inhibition and a less usual metallic organic framework nanozyme was employed, MOF-818 with catechol oxidase-like activity. The performance of the nanozyme towards the oxidation of 3,5-Di-tert-butylcatechol (3,5-DTBC) drastically improved upon confinement into the 400 nm pores of WO_3, showing a Michaelis Menten constant of 1.42 mM, a catalytic yield of 95.2% and a rate constant of 31.47 s^{-1} compared to 2.49 mM, 26% and 9.94 s^{-1}, respectively in solution. Moreover, the test integrated a signal amplification step assisted by Exo-I, as another illustration of the variety of configurations and sensing approaches enabled by the use of oligonucleotides.

Preprints (www.preprints.org) | NOT PEER-REVIEWED | Posted: 12 May 2023 doi:10.20944/preprints202305.0924.v1

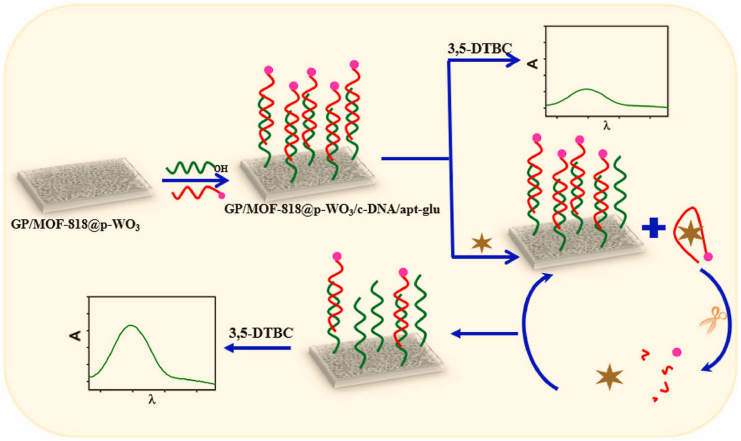

Figure 10. The assembly and working principle of the GP/MOF-818@p-WO3/c-DNA/apt-glu aptasensor for the analysis of cTnT. Reproduced from [97] with permission from Elsevier.

In more detail, a glass plate was coated with the nanozyme/p-WO_3 material and a DNA sequence, complementary to the cTnI aptamer was covalently bound to this material (Figure 10). Next, the cTnI aptamer, labeled with glutathione was anchored to the surface by hybridization to the cDNA. In the presence of 3,5-di-tert-butylcatechol (3,5-DTBC), the assembled sensor produced a low absorbance at 425 nm as the substrate's conversion was limited due to the presence of glutathione, a known inhibitor of catechol oxidase. The sensor was then incubated with the sample containing cTnI and Exo1. The aptamer, having a high affinity towards cTnI desorbed from the sensor surface while the Exo I in solution cut the aptamer and enabled the recovery of cTnI which bind further to the surface, repeating the cycle for an amplified desorption of the aptamer. In the last step the sensor was incubated again with the substrate and since the inhibition due to glutathione was removed following the desorption of the aptamer, the catalytic activity of the nanozyme was recovered. The conversion of the substrate, expressed through the increase in the absorbance at 425 nm, was proportional to the amount of desorbed aptamer and by consequence to the cTnI in the sample. Altogether this sensing configuration enabled to achieve a detection limit of 18 pg/mL cTnI [97]. While the method presumes 3 steps totaling more than 30 minutes, it was shown that it can be applied to undiluted serum samples with good accuracy (i.e., 95-107% recovery for 4 spiked samples; the analysis of the unspiked healthy serum was in agreement with results of a parallel ELISA test). Moreover, the optical aptasensor can be reused multiple times, the decrease in response after 30 uses being lower than 15% (estimated based on the data presented in [97].

To summarize, the colorimetry based approaches discussed above for the detection of CVD biomarkers reflect sustained research efforts towards (i) improving the detection sensitivity -via new nanomaterials or image processing methods, (ii) simplifying the equipment (e.g. using a smartphone as a read-out tool or measuring the width of the colored bands using a ruler, using an optical fiber amplifier), (iii) improving the stability (e.g., by replacing enzymes with nanozymes and DNAzymes), (iv) developing multiplexed platforms for the detection of multiple biomarkers relevant for the diagnosis of specific CVDs and (v) developing dual or multimodal detection strategies. New detection mechanisms (e.g using enzymatic inhibition) new labeled probes (e.g. glutathione labeled aptamer) and new aptamers were proposed. In the same time, disappointingly there was no evaluation of the stability and reproducibility of the new materials, with very few exceptions. Some lateral flow strips were evaluated and found to be stable for months at either 4ºC [98] or at room temperature[92].

The progress in the field of nanomaterials lead to increasingly more applications in sensing. In particular, major gains were related to nanoimaterials' role as catalysts (i.e, nanozymes;[94,97] in comparison with the more "traditional" use as high-loading capacity carriers for colorimetric probes or recognition molecules [87] or as signaling probes themselves [89,92].

Preprints (www.preprints.org) | NOT PEER-REVIEWED | Posted: 12 May 2023 doi:10.20944/preprints202305.0924.v1

The vast majority of reports describe the analysis of clinical samples and their comparison with current procedures implemented in clinical laboratories (Table 2). Some works were limited to the analysis of a few samples of spiked serum, indicative of applicative potential and adequate accuracy of the new methods for CBD diagnosis. Nonetheless, many of the studies went further to include the application of the new methods for testing a few up to 50 patient samples [90]. Particularly remarkable are reports on multiplexed detection of several biomarkers targeting the diagnostic of specific CVD diseases (see the review of [9] which include data on their diagnostic accuracy [90] . This trend is encouraging for the future development of the proposed methods into commercial kits and devices.

3.6. Other Optical Methods

Retroreflection is an optical phenomenon that consists in the reflection of the incident light back to the light source by a specific surface called "retroreflector". This optical phenomenon, widely exploited to make traffic signs and reflective tape for clothing was considered recently for signal transduction in the biosensors field [99-101]. The use of polychromatic instead of monochromatic light reduces costs of the optical detection while the compatibility with the smartphone LED flash and camera is an additional huge asset of retroreflection devices. Thus, it enables to simplify the needed equipment e.g., by integrating both the light generation and the detection parts in a smartphone. Microsized retroreflective surfaces that can function as optical signal labels in biosensors were devised from Janus particles, e.g silica spheres with one hemisphere coated with a retroflective layer, made by successive deposition of aluminum and gold layers [99-101]. A 2022 report by Kim et al [101] describes a microfluidic chip used with retroreflective particles for the detection of CK-MB in spiked serum by an approach that circumvents the washing steps. The capture antibody is anchored on the transparent microfluidic chip. The detection antibody is specifically attached to the silica half-sphere of Janus particles, as the gold coated hemisphere of the Janus particles was first blocked with 6-mercaptohexanol. The biomarker, CK-MB gets "sandwiched" between the capture and the detection antibody. By flipping the microfluidic chip the unbound Janus particles get sedimented away from the chip's surface. This ingenious, wash free approach enabled the user-friendly detection of CK MB in 1 h using a device integrating a smartphone.

The formation of particle aggregates facilitated by the binding of a target biomarker stands at the base of some alternative approaches for the detection of CVD biomarkers. The aggregates' formation influences the light scattering properties and turbidity of the solution. Based on this principle, the detection of NT-proBNP was achieved in under 20 minutes, down to 7.4 fg/mL by dynamic light scattering [102]. The test relies on the use of (i) magnetic beads modified with antibodies specific for NT-proBNP and (ii) silica particles modified with 3-aminophenylboronic acid. Aggregates of the two kinds of particles are formed In the presence of NT-proBNP, binding both to the magnetic beads (via the antibody) and to the silica nanoparticles (by boronate affinity). The hydrodynamic diameter of the aggregates varies linearly with the concentration of NT-proBNP in the range from 12 fg/mL to 100 ng/mL. The selectivity of the assay was first proven with a set of monosaccharides and glycoproteins, after which the test was applied for the analysis of a set of 40 clinical samples. Moreover, the results were compared with a standard time resolved fluorescence immunoassay (TRFIA) used in the clinical laboratories. The sensitivity for NT-proBNP was better than that of the standard assay and the results were linearly correlated to those provided by the standard method (correlation coefficient: 0.9745), indicating that the proposed assay is accurate and adequate for clinical samples. Notably, the assay requires a very low volume of sample (1 μL).

Microfiber Bragg grating (mFBG) probes have a good potential to be used for in vivo and at-patient monitoring of biomarkers, due to their sensitivity, compactness and multiplexing possibilities [103]. A FBG is an optical fiber in which the refraction index changes in the longitudinal axis, enabling in essence to modulate what wavelengths will be reflected and what will be transmitted by the fiber. Towards advancing from the theory to practice, Ran et al developed a harmonic optical mFBG immunosensor for the detection for cTnI [103] based on a fiber functionalized with a specific antibody. The difference in the reflection spectrum acquired at the 2nd and 3rd harmonic resonances

 doi:10.20944/preprints202305.0924.v1

enabled to distinguish between the temperature effect and the specific sensor signal. Owing to the faster binding kinetics at higher temperature the detection of cTnI in serum can be significantly shortened, from 1h to 25 min if the measurements are performed at 37º C rather than at 25º C.

4. Challenges in the Development of Optical Biosensors for CVD

The major hurdles in the development of optical biosensors for CVD are related to proving the performances of the new analytical tools by analyzing large sets of clinical samples and comparing with standard methods in clinical laboratories. This is the critical step for launching the proposed devices and methods towards commercial applications and widespread adoption. However, until then, there are some smaller but very important issues to address, such as the assessment of specificity and accuracy of the proposed methods.

A brief look at the specificity studies summarized in Tables 1 and 2 shows the large variations between studies with respect to the number of potentially interfering molecules that were evaluated. Moreover, their quantitative ratio compared to the target analyte was also very variable among the studies and did not always reflect the actual ratios expected in the biological samples. With concern to proving accuracy, this was often evaluated exclusively based on spiked serum samples and the calculated recovery was excellent, with several concentration levels often evaluated in the same study. This is an important achievement, nonetheless, analyzing a set of different samples, large enough to reflect differences in the sample composition, not only with respect of the target analyte but the matrix itself, would be more convincing. A practical problem that is evidenced when looking closer at the spiking protocols is the incorrect manner still used by some researchers, where the sample (serum) was first diluted and then spiked, instead of spiking first and then performing any sample pre-treatment including dilution. These examples highlight the need for adhering to uniform, adequate experimental protocols for evaluating the specificity and accuracy of the proposed biosensors and assays.

Reconciling the analysis of several biomarkers with a small sample size is another challenge that could be addressed by novel, high sensitivity biosensors and assays.

Salivary biomarkers are increasingly researched in the quest for establishing less invasive analysis procedures [104]. Nonetheless, so far, the number of studies focused on testing CVD biomarkers in saliva is small, the number of samples analyzed is also low and those analyzed in parallel to blood samples is even fewer. Consequently, there are no clear established correlations with blood levels of the same biomarkers. The analysis of saliva remains difficult due to the exquisite sensitivity of the methods require to accurately analyze the samples (levels being even 1000 times lower than in blood and also due to several factors of variation. So far, there were some indications that natriuretic peptides are useful indicators of heart failure. Recent studies validated the use of reference methods such as ELISA and established the stability of saliva samples. As noted by Rammos et al [104] a panel of several biomarkers, rather than the analysis of individual compounds will provide a good correlation with standard methods that use blood as sampling matrix and thus will promote the acceptance of saliva testing in the medical community. Nonetheless, more and larger studies need to pe conducted to obtain statistically relevant data.

5. Conclusions and Perspectives

The field of optical biosensors progressed at a fast pace aiming to the development of ever more specific and sensitive, faster and more convenient devices, i.e., simpler and cheaper. Multiplexed detection was increasingly researched as a solution facilitating faster diagnosis and monitoring of specific CVDs.

Several solutions were advanced to shorten the time per assay, including e.g., by conducting the measurements at higher temperature for faster binding kinetics. Progress was also made with respect of improving the portability of the equipment, for its simplification and costs reduction.

Other advancements were directed to making the tests less invasive to encourage patient compliance. The strategies pursued varied from reducing the sample volume per test to a few μL (similar to glucose tests) to using alternative sample matrices such as saliva.

The current wealth of knowledge enabled also to set new ambitious goals for the future. In perspective:

- new biomarkers or combinations of biomarkers will be proposed as relevant for CVD; their discovery and determination will involve a huge amount of data whose interpretation can be facilitated by artificial intelligence (machine learning) approaches
- new biorecognition receptors await discovery, in particular it can be anticipated that more stable aptamers, MIPs together with nanobodies will be screened for their specificity towards established or new biomarkers. With regards to aptamers, DNA amplification and editing techniques will likely see increased application in the optical sensing of CVD biomarkers.
- continuous development of optical readers and disposable tests with fast reading will enable to lower the prices and simplify to the point of facilitating at home testing- similar to glucose testing for diabetic persons.

Author Contributions: Conceptualization, A.V., C.P, M.I and M.P; methodology, S.D, S.A; writing—original draft preparation, R.M.B, C.P, S.D, A.V, M.I, M.P.; writing—review and editing, A.V., C.P, M.I, M.P, S.A. All authors have read and agreed to the published version of the manuscript.

Funding: This work was supported by a grant of the Ministry of Research, Innovation and Digitization, CCCDI – UEFISCDI, project number PN-III-P2-2.1-PED-2021-1998, within PNCDI III (for MP, SA, AV), PN-III-P4-ID-PCE-2020-2297 (for RMB) and PN-III-P2-2.1-PED-2019-4934, ERANET-M (SmartMatter, 173), PN-III-P2-2.1-PED-2021-3090, ERANET-PERMED-POC4Allergies, PN-III-P4-ID-PCE-2020-2432, PN-III-P4-ID-PCE-2020-1433, PN-III-P4-PCE-2021-1281 (for CP and SD)..

Institutional Review Board Statement: Not applicable.

Informed Consent Statement: Not applicable.

Data Availability Statement:. Data sharing not applicable.

Conflicts of Interest: The authors declare no conflict of interest.

References

1. Sharma, A.; Jang, J. Flexible electrical aptasensor using dielectrophoretic assembly of graphene oxide and its subsequent reduction for cardiac biomarker detection. *Sci, Rep.* **2019**, *9*, 5970, doi:10.1038/s41598-019-42506-1.
2. World Health Organisation, Available online: https://www.who.int/health-topics/cardiovascular-diseases#tab=tab_1 (accessed on May 8, 2023).
3. World Health Organisation, Available online: https://www.who.int/news-room/fact-sheets/detail/cardiovascular-diseases-(cvds) (accessed on May 8, 2023).
4. Knuuti, J.; Wijns, W.; Saraste, A.; Capodanno, D.; Barbato, E.; Funck-Brentano, C.; Prescott, E.; Storey, R.F.; Deaton, C.; Cuisset, T.; et al. 2019 ESC Guidelines for the diagnosis and management of chronic coronary syndromes: The Task Force for the diagnosis and management of chronic coronary syndromes of the European Society of Cardiology (ESC). *Eur. Heart J.* **2020**, *41*, 407-477, doi:10.1093/eurheartj/ehz425.
5. McDonagh, T.A.; Metra, M.; Adamo, M.; Gardner, R.S.; Baumbach, A.; Böhm, M.; Burri, H.; Butler, J.; Čelutkienė, J.; Chioncel, O.; et al. 2021 ESC Guidelines for the diagnosis and treatment of acute and chronic heart failure: Developed by the Task Force for the diagnosis and treatment of acute and chronic heart failure of the European Society of Cardiology (ESC) With the special contribution of the Heart Failure Association (HFA) of the ESC. *Eur. Heart J.* **2021**, *42*, 3599-3726, doi:10.1093/eurheartj/ehab368.
6. Abensur Vuillaume, L.; Frija-Masson, J.; Hadjiat, M.; Riquier, T.; d'Ortho, M.-P.; Le Borgne, P.; Goetz, C.; Voss, P.L.; Ougazzaden, A.; Salvestrini, J.-P.; et al. Biosensors for the Rapid Detection of Cardiovascular Biomarkers of Vital Interest: Needs, Analysis and Perspectives. *J Pers Med.* **2022**, *12*, 1942, doi: 10.3390/jpm12121942.
7. Collinson, P. Cardiac biomarker measurement by point of care testing - Development, rationale, current state and future developments. *Clin. Chim. Acta* **2020**, *508*, 234-239, doi:10.1016/j.cca.2020.05.018.
8. Szunerits, S.; Mishyn, V.; Grabowska, I.; Boukherroub, R. Electrochemical cardiovascular platforms: Current state of the art and beyond. *Biosens. Bioelectron.* **2019**, *131*, 287-298, doi:10.1016/j.bios.2019.02.010.
9. Mani, V.; Durmus, C.; Khushaim, W.; Ferreira, D.C.; Timur, S.; Arduini, F.; Salama, K.N. Multiplexed sensing techniques for cardiovascular disease biomarkers - A review. *Biosens. Bioelectron.* **2022**, *216*, 114680, doi:10.1016/j.bios.2022.114680.

10. Iqubal, A.; Khan, A.; Laeeq, A.; Malhotra, K.; Ansari, M.A.; Haque, S.E. Recent Updates on Current and Upcoming Biomarkers for Cardiovascular Diseases. *Curr. Pharm. Des.* **2021**, *27*, 3881-3900, doi:10.2174/1381612827666210224143047.
11. Navarro, C.; Fishlock, S.J.; Steele, D.N.; Puttaswamy, S.V.; Lubarsky, G.; Raj, S.; Mclaughlin, J. A Point-of-Care Measurement of NT-proBNP for Heart Failure Patients. *IEEE Access* **2020**, *8*, 138973-138983, doi:10.1109/ACCESS.2020.3007988.
12. Titus, J.; Wu, A.H.B.; Biswal, S.; Burman, A.; Sengupta, S.P.; Sengupta, P.P. Development and preliminary validation of infrared spectroscopic device for transdermal assessment of elevated cardiac troponin. *Commun. Med.* **2022**, *2*, doi:10.1038/s43856-022-00104-9.
13. Moe, K.T.; Wong, P. Current trends in diagnostic biomarkers of acute coronary syndrome. *Ann. Acad. Med. Singap.* **2010**, *39*, 210-215, doi: 10.47102/annals-acadmedsg.V39N3p210.
14. Stone, M.J.; Waterman, M.R.; Harimoto, D.; Murray, G.; Willson, N.; Platt, M.R.; Blomqvist, G.; Willerson, J.T. Serum myoglobin level as diagnostic test in patients with acute myocardial infarction. *Br. Heart J.* **1977**, *39*, 375-380, doi:10.1136/hrt.39.4.375.
15. John, R.V.; Devasiya, T.; V, R.N.; Adigal, S.; Lukose, J.; Kartha, V.B.; Chidangil, S. Cardiovascular biomarkers in body fluids: progress and prospects in optical sensors. *Biophys. Rev.* **2022**, *14*, 1023-1050, doi:10.1007/s12551-022-00990-2.
16. Qureshi, A.; Gurbuz, Y.; Niazi, J.H. Biosensors for cardiac biomarkers detection: A review. *Sens. Actuators B Chem.* **2012**, *171-172*, 62-76, doi:10.1016/j.snb.2012.05.077.
17. Cabaniss, C.D. Creatinine kinase. In *Clinical Methods: The History, Physical, and Laboratory Examinations. 3rd edition.*, Walker HK, H.W., Hurst JW, editors., Ed.; Butterworths;: Boston, 1990.
18. Gomes, A.V.; Potter, J.D.; Szczesna-Cordary, D. The role of troponins in muscle contraction. *IUBMB Life* **2002**, *54*, 323-333, doi:10.1080/15216540216037.
19. Apple, F.S.; Pearce, L.A.; Smith, S.W.; Kaczmarek, J.M.; Murakami, M.M. Role of monitoring changes in sensitive cardiac troponin I assay results for early diagnosis of myocardial infarction and prediction of risk of adverse events. *Clin. Chem.* **2009**, *55*, 930-937, doi:10.1373/clinchem.2008.114728.
20. Noh, S.; Kim, J.; Kim, G.; Park, C.; Jang, H.; Lee, M.; Lee, T. Recent Advances in CRP Biosensor Based on Electrical, Electrochemical and Optical Methods. *Sensors* **2021**, *21*, doi:10.3390/s21093024.
21. Castro, A.R.; Silva, S.O.; Soares, S.C. The Use of High Sensitivity C-Reactive Protein in Cardiovascular Disease Detection. *J. Pharm. Pharm. Sci.* **2018**, *21*, 496-503, doi:10.18433/jpps29872.
22. Goryacheva, O.A.; Ponomaryova, T.D.; Drozd, D.D.; Kokorina, A.A.; Rusanova, T.Y.; Mishra, P.K.; Goryacheva, I.Y. Heart failure biomarkers BNP and NT-proBNP detection using optical labels. *TrAC - Trends Analyt. Chem.* **2022**, *146*, 116477, doi: 10.1016/j.trac.2021.116477.
23. Palazzuoli, A.; Gallotta, M.; Quatrini, I.; Nuti, R. Natriuretic peptides (BNP and NT-proBNP): measurement and relevance in heart failure. *Vas. Health Risk Manag.* **2010**, *6*, 411-418, doi:10.2147/vhrm.s5789.
24. Chow, S.L.; Maisel, A.S.; Anand, I.; Bozkurt, B.; de Boer, R.A.; Felker, G.M.; Fonarow, G.C.; Greenberg, B.; Januzzi, J.L.; Kiernan, M.S.; et al. Role of Biomarkers for the Prevention, Assessment, and Management of Heart Failure: A Scientific Statement From the American Heart Association. *Circulation* **2017**, *135*, e1054-e1091, doi:10.1161/CIR.0000000000000490.
25. Komarova, N.; Panova, O.; Titov, A.; Kuznetsov, A. Aptamers Targeting Cardiac Biomarkers as an Analytical Tool for the Diagnostics of Cardiovascular Diseases: A Review. *Biomedicines* **2022**, *10*, doi:10.3390/biomedicines10051085.
26. Collier, P.; Watson, C.J.; Voon, V.; Phelan, D.; Jan, A.; Mak, G.; Martos, R.; Baugh, J.A.; Ledwidge, M.T.; McDonald, K.M. Can emerging biomarkers of myocardial remodelling identify asymptomatic hypertensive patients at risk for diastolic dysfunction and diastolic heart failure? *Eur. J. Heart Fail.* **2011**, *13*, 1087-1095, doi:10.1093/eurjhf/hfr079.
27. Crapnell, R.D.; Dempsey, N.C.; Sigley, E.; Tridente, A.; Banks, C.E. Electroanalytical point-of-care detection of gold standard and emerging cardiac biomarkers for stratification and monitoring in intensive care medicine - a review. *Mikrochim. Acta* **2022**, *189*, 142, doi:10.1007/s00604-022-05186-9.
28. Masson, J.-F. Surface Plasmon Resonance Clinical Biosensors for Medical Diagnostics. *ACS Sens.* **2017**, *2*, 16-30, doi:10.1021/acssensors.6b00763.
29. David, S.; Gheorghiu, M.; Daakour, S.; Munteanu, R.E.; Polonschii, C.; Gáspár, S.; Barboiu, M.; Gheorghiu, E. Real Time SPR Assessment of the Structural Changes of Adaptive Dynamic Constitutional Frameworks as a New Route for Sensing. Materials (Basel, Switzerland) 2022, 15, doi:10.3390/ma15020483.
30. Homola, J. Surface Plasmon Resonance Sensors for Detection of Chemical and Biological Species. *Chem. Rev.* **2008**, *108*, 462-493, doi:10.1021/cr068107d.
31. Nakagawa, H.; Saito, I.; Chinzei, T.; Nakaoki, Y.; Iwata, Y. The merits/demerits of biochemical reaction measurements by SPR reflectance signal at a fixed angle. *Sens. Actuators B: Chem.* **2005**, *108*, 772-777, doi:10.1016/j.snb.2004.12.034.

32. Çimen, D.; Bereli, N.; Günaydın, S.; Denizli, A. Detection of cardiac troponin-I by optic biosensors with immobilized anti-cardiac troponin-I monoclonal antibody. *Talanta* **2020**, *219*, 121259, doi: 10.1016/j.talanta.2020.121259.
33. Che JX, W.Y., Chang SJ, Chen CJ, Liu JT. Peptide-based antifouling aptasensor for cardiac troponin I detection by surface plasmon resonance applied in medium sized Myocardial Infarction. *Ann Biomed Sci Eng* **2020**, *4*, 001-008, doi:10.29328/journal.abse.1001007.
34. Krupin, O.; Berini, P. Long-Range Surface Plasmon-Polariton Waveguide Biosensors for Human Cardiac Troponin I Detection. *Sensors* **2019**, *19*, doi:10.3390/s19030631.
35. Liyanage, T.; Sangha, A.; Sardar, R. Achieving biosensing at attomolar concentrations of cardiac troponin T in human biofluids by developing a label-free nanoplasmonic analytical assay. *Analyst* **2017**, *142*, 2442-2450, doi:10.1039/C7AN00430C.
36. Assunção, A.S.; M, V.; M., L.; C., C.; F.M, C.; J., M.-B.; C., M.; S.O, P.; C., L. Towards heart failure biomarker detection with plasmonic fiber tip biosensors. In Proceedings of the 2022 IEEE International Symposium on Medical Measurements and Applications (MeMeA), 22-24 June 2022, 2022; pp. 1-5.
37. Wu, Q.; Sun, Y.; Zhang, D.; Li, S.; Zhang, Y.; Ma, P.; Yu, Y.; Wang, X.; Song, D. Ultrasensitive magnetic field-assisted surface plasmon resonance immunoassay for human cardiac troponin I. *Biosens. Bioelectron.* **2017**, *96*, 288-293, doi:10.1016/j.bios.2017.05.023.
38. Zhao, J.; Liang, D.; Gao, S.; Hu, X.; Koh, K.; Chen, H. Analyte-resolved magnetoplasmonic nanocomposite to enhance SPR signals and dual recognition strategy for detection of BNP in serum samples. *Biosens. Bioelectron.* **2019**, *141*, 111440, doi:10.1016/j.bios.2019.111440.
39. Harpaz, D.; Koh, B.; Marks, R.S.; Seet, R.C.S.; Abdulhalim, I.; Tok, A.I.Y. Point-of-Care Surface Plasmon Resonance Biosensor for Stroke Biomarkers NT-proBNP and S100β Using a Functionalized Gold Chip with Specific Antibody. Sensors (Basel, Switzerland) 2019, 19, doi:10.3390/s19112533.
40. Ricardo, A. *Surface-Enhanced Vibrational Spectroscopy*; 2006.
41. Monica Baia, S.A., Traian Iliescu. *Raman and SERS Investigations of Pharmaceuticals*, 1 ed.; Springer Berlin, Heidelberg: 2008; pp. XIII, 214.
42. Nagy-Simon, T.; Hada, A.-M.; Suarasan, S.; Potara, M. Recent advances on the development of plasmon-assisted biosensors for detection of C-reactive protein. *J. Mol. Struct.* **2021**, *1246*, 131178, doi: 10.1016/j.molstruc.2021.131178.
43. Benford, M.; Wang, M.; Kameoka, J.; Coté, G. *Detection of cardiac biomarkers exploiting surface enhanced Raman scattering (SERS) using a nanofluidic channel based biosensor towards coronary point-of-care diagnostics*; SPIE: 2009; Volume 7192.
44. Benford, M.; Wang, M.; Kameoka, J.; Good, T.; Cote, G. *Functionalized nanoparticles for measurement of biomarkers using a SERS nanochannel platform*; SPIE: 2010; Volume 7577.
45. Yu, Z.; Chen, L.; Wang, Y.; Wang, X.; Song, W.; Ruan, W.; Zhao, B.; Cong, Q. A SERS-active enzymatic product used for the quantification of disease-related molecules. *J. Raman Spectrosc.* **2014**, *45*, 75-81, doi: 10.1002/jrs.4425.
46. Coté, G.; Kameoka, J.; Marks, H. *Using micro and nanofluidics with surface enhanced Raman spectroscopy for in vitro blood based biomarker detection*; SPIE: 2014; Volume 9155.
47. Garza, J.; Cote, G. *Design of Raman active nanoparticles for SERS-based detection*; SPIE: 2016; Volume 9722.
48. El-Said, W.A.; Fouad, D.M.; El-Safty, S.A. Ultrasensitive label-free detection of cardiac biomarker myoglobin based on surface-enhanced Raman spectroscopy. *Sens. Actuators B: Chem.* **2016**, *228*, 401-409, doi: 10.1016/j.snb.2016.01.041.
49. Gao, R.; Chen, F.; Yang, D.; Zheng, L.; Jing, T.; Jia, H.; Chen, X.; Lu, Y.; Xu, S.; Zhang, D.; et al. Simultaneous SERS-based immunoassay of dual cardiac markers on pump-free hybrid microfluidic chip. *Sens. Actuators B: Chem.* **2022**, *369*, 132378, doi:10.1016/j.snb.2022.132378.
50. Bai, T.; Wang, M.; Cao, M.; Zhang, J.; Zhang, K.; Zhou, P.; Liu, Z.; Liu, Y.; Guo, Z.; Lu, X. Functionalized Au@Ag-Au nanoparticles as an optical and SERS dual probe for lateral flow sensing. *Anal. Bioanal. Chem.* **2018**, *410*, 2291-2303, doi:10.1007/s00216-018-0850-z.
51. Zhang, D.; Huang, L.; Liu, B.; Ni, H.; Sun, L.; Su, E.; Chen, H.; Gu, Z.; Zhao, X. Quantitative and ultrasensitive detection of multiplex cardiac biomarkers in lateral flow assay with core-shell SERS nanotags. *Biosens. Bioelectron.* **2018**, *106*, 204-211, doi:10.1016/j.bios.2018.01.062.
52. Zhang, D.; Huang, L.; Liu, B.; Su, E.; Chen, H.-Y.; Gu, Z.; Zhao, X. Quantitative detection of multiplex cardiac biomarkers with encoded SERS nanotags on a single T line in lateral flow assay. *Sens. Actuators B: Chem.* **2018**, *277*, 502-509, doi:10.1016/j.snb.2018.09.044.
53. Cheng, Z.; Wang, R.; Xing, Y.; Zhao, L.; Choo, J.; Yu, F. SERS-based immunoassay using gold-patterned array chips for rapid and sensitive detection of dual cardiac biomarkers. *Analyst* **2019**, *144*, 6533-6540, doi:10.1039/C9AN01260E.
54. Su, Y.; Xu, S.; Zhang, J.; Chen, X.; Jiang, L.-P.; Zheng, T.; Zhu, J.-J. Plasmon Near-Field Coupling of Bimetallic Nanostars and a Hierarchical Bimetallic SERS "Hot Field": Toward Ultrasensitive Simultaneous

Detection of Multiple Cardiorenal Syndrome Biomarkers. *Anal. Chem.* **2019**, *91*, 864-872, doi:10.1021/acs.analchem.8b03573.
55. Khlebtsov, B.N.; Bratashov, D.N.; Byzova, N.A.; Dzantiev, B.B.; Khlebtsov, N.G. SERS-based lateral flow immunoassay of troponin I by using gap-enhanced Raman tags. *Nano Res.* **2019**, *12*, 413-420, doi:10.1007/s12274-018-2232-4.
56. Tu, D.; Holderby, A.; Guo, H.; Mabbott, S.; Tian, L.; Coté, G.L. Spectrally multiplexed assay using gap enhanced nanoparticle for detection of a myocardial infarction biomarker panel. *Anal. Chim. Acta* **2022**, *1198*, 339562, doi:10.1016/j.aca.2022.339562.
57. Tu, D.; Holderby, A.; Coté, G.L. Aptamer-based surface-enhanced resonance Raman scattering assay on a paper fluidic platform for detection of cardiac troponin I. *J. Biomed. Opt.* **2020**, *25*, doi:10.1117/1.Jbo.25.9.097001.
58. Lim, W.Y.; Goh, C.-H.; Thevarajah, T.M.; Goh, B.T.; Khor, S.M. Using SERS-based microfluidic paper-based device (μPAD) for calibration-free quantitative measurement of AMI cardiac biomarkers. *Biosens. Bioelectron.* **2020**, *147*, 111792, doi:10.1016/j.bios.2019.111792.
59. Chon, H.; Lee, S.; Yoon, S.Y.; Lee, E.K.; Chang, S.I.; Choo, J. SERS-based competitive immunoassay of troponin I and CK-MB markers for early diagnosis of acute myocardial infarction. *Chem. Commun. (Camb.)* **2014**, *50*, 1058-1060, doi:10.1039/c3cc47850e.
60. He, Y.; Wang, Y.; Yang, X.; Xie, S.; Yuan, R.; Chai, Y. Metal Organic Frameworks Combining CoFe2O4 Magnetic Nanoparticles as Highly Efficient SERS Sensing Platform for Ultrasensitive Detection of N-Terminal Pro-Brain Natriuretic Peptide. *ACS Appl. Mater. Interfaces* **2016**, *8*, 7683-7690, doi:10.1021/acsami.6b01112.
61. Zheng, D.; Wang, Z.; Wu, J.; Li, S.; Li, W.; Zhang, H.; Xia, L. A Raman immunosensor based on SERS and microfluidic chip for all-fiber detection of brain natriuretic peptide. *Infrared Phys. Technol.* **2022**, *125*, 104252, doi:10.1016/j.infrared.2022.104252.
62. Fu, X.; Wang, Y.; Liu, Y.; Liu, H.; Fu, L.; Wen, J.; Li, J.; Wei, P.; Chen, L. A graphene oxide/gold nanoparticle-based amplification method for SERS immunoassay of cardiac troponin I. *Analyst* **2019**, *144*, 1582-1589, doi:10.1039/C8AN02022A.
63. Wen, X.; Ou, Y.-C.; Zarick, H.F.; Zhang, X.; Hmelo, A.B.; Victor, Q.J.; Paul, E.P.; Slocik, J.M.; Naik, R.R.; Bellan, L.M.; et al. PRADA: Portable Reusable Accurate Diagnostics with nanostar Antennas for multiplexed biomarker screening. *Bioeng. Transl. Med.* **2020**, *5*, e10165, doi:10.1002/btm2.10165.
64. Hu, C.; Ma, L.; Mi, F.; Guan, M.; Guo, C.; Peng, F.; Sun, S.; Wang, X.; Liu, T.; Li, J. SERS-based immunoassay using core–shell nanotags and magnetic separation for rapid and sensitive detection of cTnI. *New J. Chem.* **2021**, *45*, 3088-3094, doi:10.1039/D0NJ05774F.
65. Hu, C.; Ma, L.; Guan, M.; Mi, F.; Peng, F.; Guo, C.; Sun, S.; Wang, X.; Liu, T.; Li, J. SERS-based magnetic immunoassay for simultaneous detection of cTnI and H-FABP using core–shell nanotags. *Anal. Methods* **2020**, *12*, 5442-5449, doi:10.1039/D0AY01564D.
66. Lee, H.; Youn, H.; Hwang, A.; Lee, H.; Park, J.Y.; Kim, W.; Yoo, Y.; Ban, C.; Kang, T.; Kim, B. Troponin Aptamer on an Atomically Flat Au Nanoplate Platform for Detection of Cardiac Troponin I. *Nanomaterials (Basel, Switzerland)* **2020**, *10*, doi:10.3390/nano10071402.
67. Wang, J.; Xu, C.; Lei, M.; Ma, Y.; Wang, X.; Wang, R.; Sun, J.; Wang, R. Microcavity-based SERS chip for ultrasensitive immune detection of cardiac biomarkers. *Microchem. J.* **2021**, *171*, 106875, doi: 10.1016/j.microc.2021.106875.
68. Ji, T.; Xu, X.; Wang, X.; Zhou, Q.; Ding, W.; Chen, B.; Guo, X.; Hao, Y.; Chen, G. Point of care upconversion nanoparticles-based lateral flow assay quantifying myoglobin in clinical human blood samples. *Sens. Actuators B: Chem.* **2019**, *282*, 309-316, doi:10.1016/j.snb.2018.11.074.
69. Li, J.; Lv, Y.; Li, N.; Wu, R.; Li, J.; You, J.; Shen, H.; Chen, X.; Li, L.S. Dual protecting encapsulation synthesis of ultrastable quantum-dot nanobeads for sensitive and accurate detection of cardiac biomarkers. *Sens. Actuators B: Chem.* **2021**, *344*, 130275, doi:10.1016/j.snb.2021.130275.
70. Chen, J.; Ran, F.; Chen, Q.; Luo, D.; Ma, W.; Han, T.; Wang, C.; Wang, C. A fluorescent biosensor for cardiac biomarker myoglobin detection based on carbon dots and deoxyribonuclease I-aided target recycling signal amplification. *RSC Advances* **2019**, *9*, 4463-4468, doi:10.1039/C8RA09459D.
71. Lee, K.W.; Kim, K.R.; Chun, H.J.; Jeong, K.Y.; Hong, D.-K.; Lee, K.-N.; Yoon, H.C. Time-resolved fluorescence resonance energy transfer-based lateral flow immunoassay using a raspberry-type europium particle and a single membrane for the detection of cardiac troponin I. *Biosens. Bioelectron.* **2020**, *163*, 112284, doi: 10.1016/j.bios.2020.112284.
72. Ali, G.K.; Omer, K.M. Ultrasensitive aptamer-functionalized Cu-MOF fluorescent nanozyme as an optical biosensor for detection of C-reactive protein. *Anal. Biochem.* **2022**, *658*, 114928, doi:10.1016/j.ab.2022.114928.
73. Tu, A.; Shang, J.; Wang, Y.; Li, D.; Liu, L.; Gan, Z.; Yin, Y.; Zhang, P. Detection of B-type natriuretic peptide by establishing a low-cost and replicable fluorescence resonance energy transfer platform. *Mikrochim. Acta* **2020**, *187*, 331, doi:10.1007/s00604-020-04247-1.

74. Sullivan, M.V.; Stockburn, W.J.; Hawes, P.C.; Mercer, T.; Reddy, S.M. Green synthesis as a simple and rapid route to protein modified magnetic nanoparticles for use in the development of a fluorometric molecularly imprinted polymer-based assay for detection of myoglobin. *Nanotechnology* **2021**, *32*, 095502, doi:10.1088/1361-6528/abce2d.
75. Liu, D.; Zeng, Y.; Zhou, G.; Lu, X.; Miao, D.; Yang, Y.; Zhai, Y.; Zhang, J.; Zhang, Z.; Wang, H.; et al. Fluorometric determination of cardiac myoglobin based on energy transfer from a pyrene-labeled aptamer to graphene oxide. *Microchim. Acta* **2019**, *186*, 287, doi:10.1007/s00604-019-3385-x.
76. S., G.; A., M.; S., C.; M., D.; M.A, S. Detection of C-Reactive Protein using network-deployable DNA aptamer based optical nanosensor. In Proceedings of the 2019 IEEE EMBS International Conference on Biomedical & Health Informatics (BHI), 19-22 May 2019, 2019; pp. 1-4.
77. Ji, J.; Lu, W.; Zhu, Y.; Jin, H.; Yao, Y.; Zhang, H.; Zhao, Y. Porous Hydrogel-Encapsulated Photonic Barcodes for Multiplex Detection of Cardiovascular Biomarkers. *ACS Sensors* **2019**, *4*, 1384-1390, doi:10.1021/acssensors.9b00352.
78. Zhang, J.; Lv, X.; Feng, W.; Li, X.; Li, K.; Deng, Y. Aptamer-based fluorometric lateral flow assay for creatine kinase MB. *Microchim. Acta* **2018**, *185*, 364, doi:10.1007/s00604-018-2905-4.
79. Huang, L.; Zhang, Y.; Su, E.; Liu, Y.; Deng, Y.; Jin, L.; Chen, Z.; Li, S.; Zhao, Y.; He, N. Eight biomarkers on a novel strip for early diagnosis of acute myocardial infarction. *Nanoscale Adv.* **2020**, *2*, 1138-1143, doi:10.1039/C9NA00644C.
80. Piloto, A.M.L.; Ribeiro, D.S.M.; Rodrigues, S.S.M.; Santos, J.L.M.; Sampaio, P.; Sales, G. Imprinted Fluorescent Cellulose Membranes for the On-Site Detection of Myoglobin in Biological Media. *ACS Appl. Bio Mater.* **2021**, *4*, 4224-4235, doi:10.1021/acsabm.1c00039.
81. Miao, D.; Liu, D.; Zeng, Y.; Zhou, G.; Xie, W.; Yang, Y.; Wang, H.; Zhang, J.; Zhai, Y.; Zhang, Z.; et al. Fluorescent aptasensor based on D-AMA/F-CSC for the sensitive and specific recognition of myoglobin. *Spectrochim. Acta. A Mol. Biomol. Spectrosc.* **2020**, *228*, 117714, doi:10.1016/j.saa.2019.117714.
82. Gopinathan, P.; Sinha, A.; Chung, Y.-D.; Shiesh, S.-C.; Lee, G.-B. Optimization of an enzyme linked DNA aptamer assay for cardiac troponin I detection: synchronous multiple sample analysis on an integrated microfluidic platform. *Analyst* **2019**, *144*, 4943-4951, doi:10.1039/C9AN00779B.
83. Yin, B.; Wan, X.; Qian, C.; Sohan, A.S.M.M.F.; Wang, S.; Zhou, T. Point-of-Care Testing for Multiple Cardiac Markers Based on a Snail-Shaped Microfluidic Chip. *Front. Chem.* **2021**, *9*, doi:10.3389/fchem.2021.741058.
84. Dong, X.; Zhao, G.; Li, X.; Miao, J.; Fang, J.; Wei, Q.; Cao, W. Electrochemiluminescence immunoassay for the N-terminal pro-B-type natriuretic peptide based on resonance energy transfer between a self-enhanced luminophore composed of silver nanocubes on gold nanoparticles and a metal-organic framework of type MIL-125. *Mikrochim. Acta* **2019**, *186*, 811, doi:10.1007/s00604-019-3969-5.
85. Liu, X.; Zhang, H.; Qin, S.; Wang, Q.; Yang, X.; Wang, K. Optical fiber amplifier for quantitative and sensitive point-of-care testing of myoglobin and miRNA-141. *Biosens. Bioelectron.* **2019**, *129*, 87-92, doi: 10.1016/j.bios.2018.12.056.
86. António, M.; Ferreira, R.; Vitorino, R.; Daniel-da-Silva, A.L. A simple aptamer-based colorimetric assay for rapid detection of C-reactive protein using gold nanoparticles. *Talanta* **2020**, *214*, 120868, doi:10.1016/j.talanta.2020.120868.
87. Pu, Q.; Yang, X.; Guo, Y.; Dai, T.; Yang, T.; Ou, X.; Li, J.; Sheng, S.; Xie, G. Simultaneous colorimetric determination of acute myocardial infarction biomarkers by integrating self-assembled 3D gold nanovesicles into a multiple immunosorbent assay. *Mikrochim. Acta* **2019**, *186*, 138, doi:10.1007/s00604-019-3242-y.
88. Chen, M.; Zhang, J.; Peng, Y.; Bai, J.; Li, S.; Han, D.; Ren, S.; Qin, K.; Zhou, H.; Han, T.; et al. Design and synthesis of DNA hydrogel based on EXPAR and CRISPR/Cas14a for ultrasensitive detection of creatine kinase MB. *Biosens. Bioelectron.* **2022**, *218*, 114792, doi:10.1016/j.bios.2022.114792.
89. Chen, M.; Wang, Y.; Zhao, X.; Zhang, J.; Peng, Y.; Bai, J.; Li, S.; Han, D.; Ren, S.; Qin, K.; et al. Target-responsive DNA hydrogel with microfluidic chip smart readout for quantitative point-of-care testing of creatine kinase MB. *Talanta* **2022**, *243*, 123338, doi:10.1016/j.talanta.2022.123338.
90. Ozen, M.O.; Sridhar, K.; Ogut, M.G.; Shanmugam, A.; Avadhani, A.S.; Kobayashi, Y.; Wu, J.C.; Haddad, F.; Demirci, U. Total Microfluidic chip for Multiplexed diagnostics (ToMMx). *Biosens. Bioelectron.* **2020**, *150*, 111930, doi:10.1016/j.bios.2019.111930.
91. Lim, W.Y.; Thevarajah, T.M.; Goh, B.T.; Khor, S.M. Paper microfluidic device for early diagnosis and prognosis of acute myocardial infarction via quantitative multiplex cardiac biomarker detection. *Biosens. Bioelectron.* **2019**, *128*, 176-185, doi:10.1016/j.bios.2018.12.049.
92. Byzova, N.A.; Vengerov, Y.Y.; Voloshchuk, S.G.; Zherdev, A.V.; Dzantiev, A.B.B. Development of A Lateral Flow Highway: Ultra-Rapid Multitracking Immunosensor for Cardiac Markers. *Sensors (Basel, Switzerland)* **2019**, *19*, doi:10.3390/s19245494.
93. Panferov, V.G.; Byzova, N.A.; Zherdev, A.V.; Dzantiev, B.B. Peroxidase-mimicking nanozyme with surface-dispersed Pt atoms for the colorimetric lateral flow immunoassay of C-reactive protein. *Microchim. Acta* **2021**, *188*, 309, doi:10.1007/s00604-021-04968-x.

94. Xie, J.; Tang, M.-Q.; Chen, J.; Zhu, Y.-H.; Lei, C.-B.; He, H.-W.; Xu, X.-H. A sandwich ELISA-like detection of C-reactive protein in blood by citicoline-bovine serum albumin conjugate and aptamer-functionalized gold nanoparticles nanozyme. *Talanta* **2020**, *217*, 121070, doi:10.1016/j.talanta.2020.121070.
95. Torrini, F.; Palladino, P.; Brittoli, A.; Baldoneschi, V.; Minunni, M.; Scarano, S. Characterization of troponin T binding aptamers for an innovative enzyme-linked oligonucleotide assay (ELONA). *Anal. Bioanal. Chem.* **2019**, *411*, 7709-7716, doi:10.1007/s00216-019-02014-7.
96. Wang, X.; Zhang, W.; Wang, S.; Liu, W.; Liu, N.; Zhang, D. A visual cardiovascular biomarker detection strategy based on distance as readout by the coffee-ring effect on microfluidic paper. *Biochem. Eng. J.* **2021**, *176*, 108176, doi:10.1016/j.bej.2021.108176.
97. Wen, R.; Zhou, C.; Tian, J.; Lu, J. Confined catalysis of MOF-818 nanozyme and colorimetric aptasensing for cardiac troponin I. *Talanta* **2023**, *252*, 123830, doi:10.1016/j.talanta.2022.123830.
98. Poosinuntakul, N.; Chanmee, T.; Porntadavity, S.; Chailapakul, O.; Apilux, A. Silver-enhanced colloidal gold dip strip immunoassay integrated with smartphone-based colorimetry for sensitive detection of cardiac marker troponin I. *Sci. Rep.* **2022**, *12*, 19866, doi:10.1038/s41598-022-24458-1.
99. Han, Y.D.; Kim, K.R.; Lee, K.W.; Yoon, H.C. Retroreflection-based optical biosensing: From concept to applications. *Biosens. Bioelectron.* **2022**, *207*, 114202, doi:10.1016/j.bios.2022.114202.
100. Han, Y.D.; Kim, H.-S.; Park, Y.M.; Chun, H.J.; Kim, J.-H.; Yoon, H.C. Retroreflective Janus Microparticle as a Nonspectroscopic Optical Immunosensing Probe. *ACS Appl. Mater. Interfaces* **2016**, *8*, 10767-10774, doi:10.1021/acsami.6b02014.
101. Kim, K.R.; Lee, K.W.; Chun, H.J.; Lee, D.; Kim, J.-H.; Yoon, H.C. Wash-free operation of smartphone-integrated optical immunosensor using retroreflective microparticles. *Biosens. Bioelectron.* **2022**, *196*, 113722, doi:10.1016/j.bios.2021.113722.
102. Hu, J.; Ding, L.; Chen, J.; Fu, J.; Zhu, K.; Guo, Q.; Huang, X.; Xiong, Y. Ultrasensitive dynamic light scattering immunosensing platform for NT-proBNP detection using boronate affinity amplification. *J Nanobiotechnology* **2022**, *20*, 21, doi:10.1186/s12951-021-01224-5.
103. Ran, Y.; Long, J.; Xu, Z.; Yin, Y.; Hu, D.; Long, X.; Zhang, Y.; Liang, L.; Liang, H.; Guan, B.-O. Harmonic optical microfiber Bragg grating immunosensor for the accelerative test of cardiac biomarker (cTn-I). *Biosens. Bioelectron.* **2021**, *179*, 113081, doi:10.1016/j.bios.2021.113081.
104. Rammos, A.; Bechlioulis, A.; Kalogeras, P.; Tripoliti, E.E.; Goletsis, Y.; Kalivi, A.; Blathra, E.; Salvo, P.; Trivella, M.G.; Lomonaco, T.; et al. Salivary Biomarkers for Diagnosis and Therapy Monitoring in Patients with Heart Failure. A Systematic Review. *Diagnostics (Basel, Switzerland)* **2021**, *11*, doi:10.3390/diagnostics11050824.